Fundamental Interactions at Future Colliders (LFC24)
17th of September, 2024 – SISSA (Trieste, Italia)

Exotic Higgs decays at the LHC

Carlos Vázquez Sierra (LHCb/CODEX-b)
Galician Institute of High Energy Physics (IGFAE), Santiago de Compostela

IGFAE INSTITUTO GALEGO DE FÍSICA DE ALTAS ENERXÍAS 25 1999 2024

USC UNIVERSIDADE DE SANTIAGO DE COMPOSTELA · MINISTERIO DE CIENCIA, INNOVACIÓN Y UNIVERSIDADES · AGENCIA ESTATAL DE INVESTIGACIÓN · EXCELENCIA MARÍA DE MAEZTU 2024-2029 · XUNTA DE GALICIA · CENTROS CIGUS · Cofinanciado pola Unión Europea · Fondos Europeos

Is there anything beyond the Standard Model?

Indirect – deviations from SM

Is there anything beyond the Standard Model?

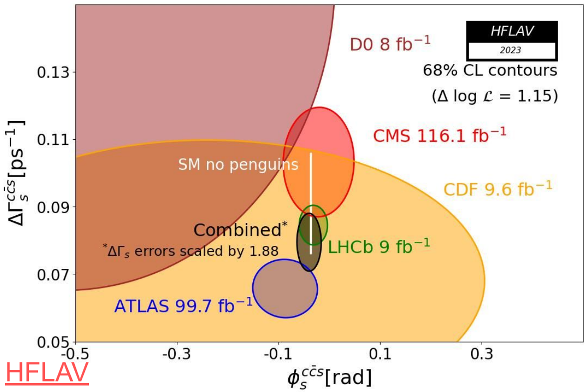

HFLAV

Is there anything beyond the Standard Model?

Indirect – deviations from SM

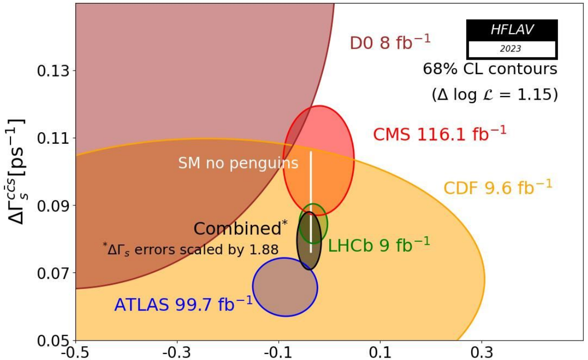

HFLAV

Direct – look for new particles

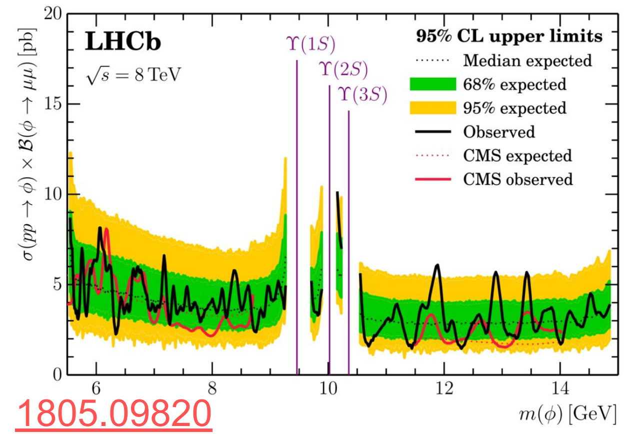

1805.09820

2405.13778

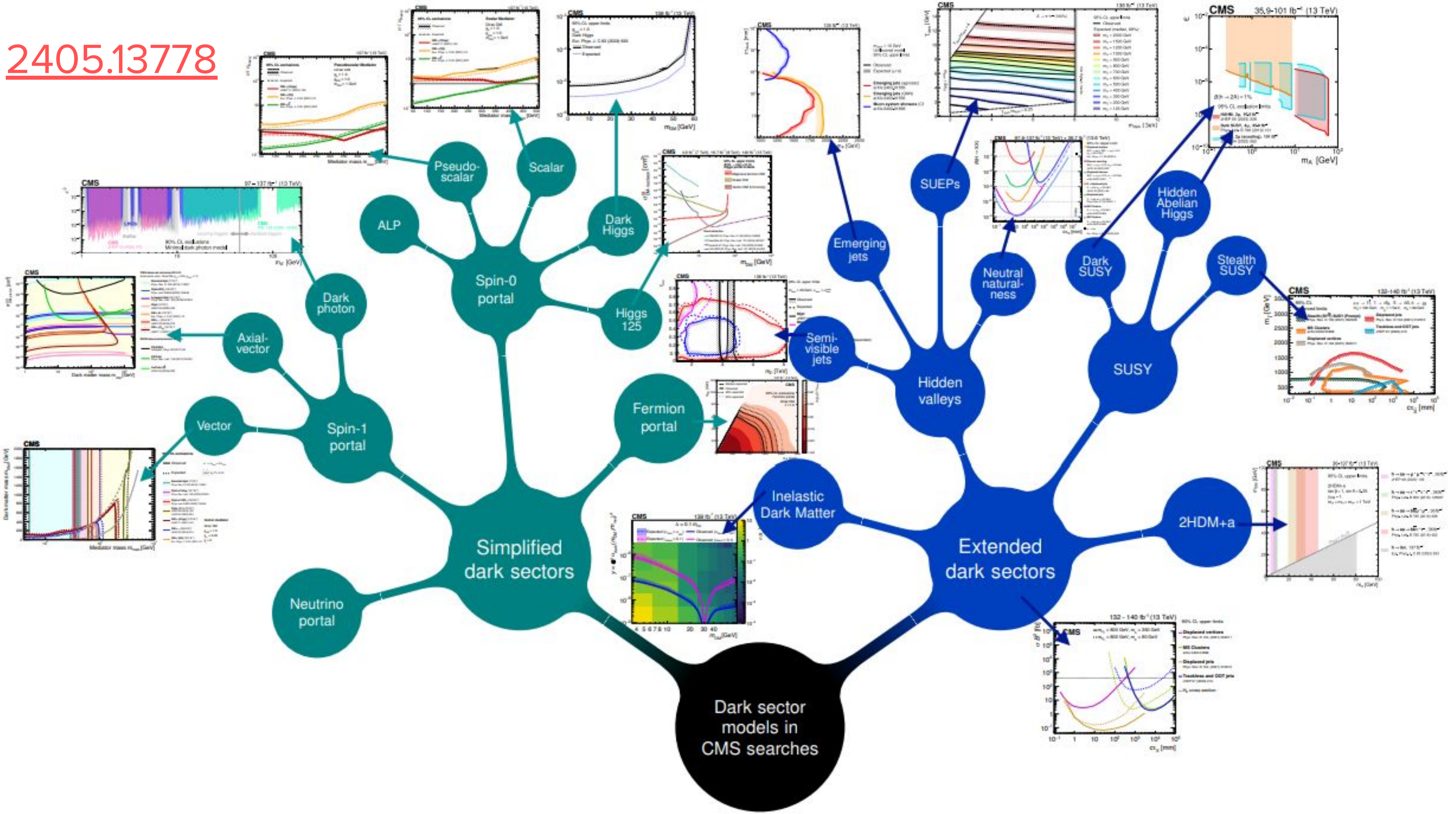

Dark sector models in CMS searches
Simplified dark sectors
Spin-0 portal
ALP
Pseudo-scalar
Scalar
Dark Higgs
Higgs 125
Spin-1 portal
Dark photon
Axial-vector
Vector
Fermion portal
Neutrino portal
Extended dark sectors
Inelastic Dark Matter
Hidden valleys
Semi-visible jets
Emerging jets
SUEPs
Neutral natural-ness
SUSY
Dark SUSY
Hidden Abelian Higgs
Stealth SUSY
2HDM+a

2405.13778

Why Exotic Higgs decays?

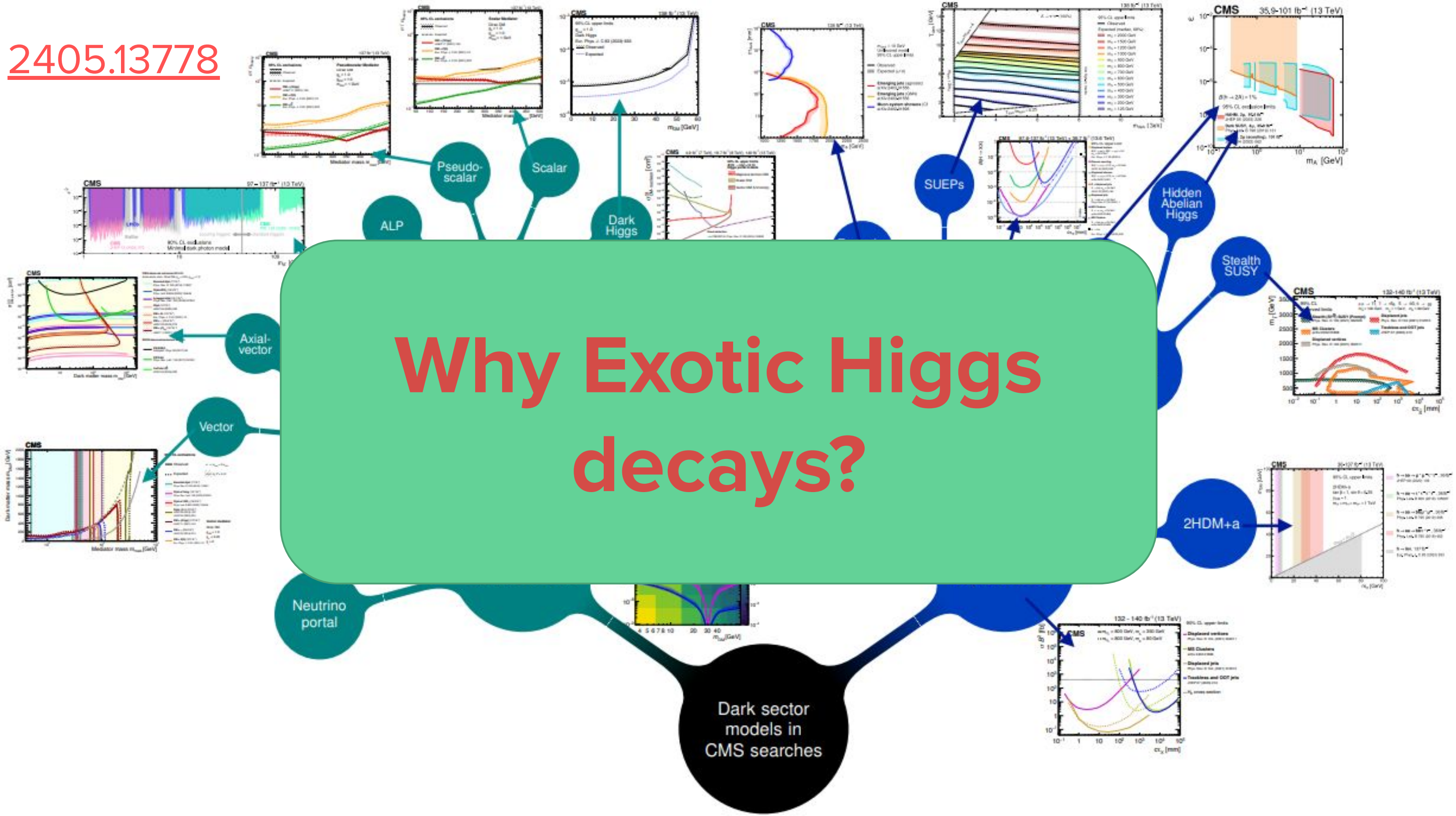

The data collected at LHC7 and LHC8 may easily contain $\mathcal{O}(50,000)$ exotic Higgs decays per experiment, $\boxed{\text{presenting us with a large discovery potential for new physics}}$, of a kind which is mostly unconstrained by existing analyses.

The data collected at LHC7 and LHC8 may easily contain $\mathcal{O}(50,000)$ exotic Higgs decays per experiment, presenting us with a large discovery potential for new physics, of a kind which is mostly unconstrained by existing analyses.

Several theoretical and experimental studies have constrained the possible Br into an invisible or an (as yet) undetected final state by fitting for the couplings of the Higgs to SM states.

The data collected at LHC7 and LHC8 may easily contain $\mathcal{O}(50,000)$ exotic Higgs decays per experiment, presenting us with a large discovery potential for new physics, of a kind which is mostly unconstrained by existing analyses.

Several theoretical and experimental studies have constrained the possible Br into an invisible or an (as yet) undetected final state by fitting for the couplings of the Higgs to SM states.

The tiny natural width of the SM Higgs boson, together with the ease with which the Higgs can mediate interactions with new physics, make exotic Higgs decays a natural and expected signature of a very broad class of theories beyond the SM.

The data collected at LHC7 and LHC8 may easily contain $\mathcal{O}(50,000)$ exotic Higgs decays per experiment, presenting us with a large discovery potential for new physics, of a kind which is mostly unconstrained by existing analyses.

Several theoretical and experimental studies have constrained the possible Br into an invisible or an (as yet) undetected final state by fitting for the couplings of the Higgs to SM states.

The tiny natural width of the SM Higgs boson, together with the ease with which the Higgs can mediate interactions with new physics, make exotic Higgs decays a natural and expected signature of a very broad class of theories beyond the SM.

the Higgs provides one of only a few "portals" that allow SM matter to interact with hidden-sector matter that is not charged under the SM forces

The data collected at LHC7 and LHC8 may easily contain $\mathcal{O}(50,000)$ exotic Higgs decays per experiment, presenting us with a large discovery potential for new physics, of a kind which is mostly unconstrained by existing analyses.

Several theoretical and experimental studies have constrained the possible Br into an invisible … Higgs to SM state…

… the ease with which … s decays a natural and expected signature of a very broad class of theories beyond the SM.

1312.4992

Exotic Decays of the 125 GeV Higgs Boson

David Curtin,[1] Rouven Essig,[1] Stefania Gori,[2,3,4] Prerit Jaiswal,[5] Andrey Katz,[6] Tao Liu,[7] Zhen Liu,[8] David McKeen,[9,10] Jessie Shelton,[6] Matthew Strassler,[6] Ze'ev Surujon,[1] Brock Tweedie,[8,11] and Yi-Ming Zhong[1,*]

the Higgs provides one of only a few "portals" that allow SM matter to interact with hidden-sector matter that is not charged under the SM forces

This talk

- $H \to aa \to 2b2\tau$ [ATLAS/CMS] Prompt
- $H \to aa \to 2b2\mu$ [CMS] Prompt
- $H \to aa \to 4\mu$ [CMS] Prompt + displaced
- $H \to aa \to 4b$ [CMS] Prompt
- $H \to aa \to 4\gamma$ [ATLAS] Prompt + displaced
- $H \to \chi\chi$ ($\chi \to 2b$) [LHCb] Displaced
- $H \to \chi\chi$ ($\chi \to e\mu\nu$) [LHCb] Displaced
- $H \to \chi\chi$ ($\chi \to \mu 2q$) [LHCb] Displaced
- $H \to Za$ ($a \to 2\gamma$) [ATLAS] Prompt
- Prospects with LHCb MS for $H \to aa \to 4\tau$

Backup:

- $H \to \chi\chi \to 4q$ [ATLAS[1,2]/CMS[1,2]] Displaced

Other results not covered here:

- $H \to aa \to 4\mu$ [ATLAS]
- $H \to aa \to 4e$ [ATLAS]
- $H \to aa \to 2e2\mu$ [ATLAS]
- $H \to aa \to 4\tau$ [CMS]
- $H \to aa \to 2\mu 2\tau$ [CMS]
- $H \to aa \to 2g2\gamma$ [ATLAS]
- $H \to Za$ ($a \to 2\gamma$) [CMS] Prompt

H → aa → 2b2τ [2407.01335]

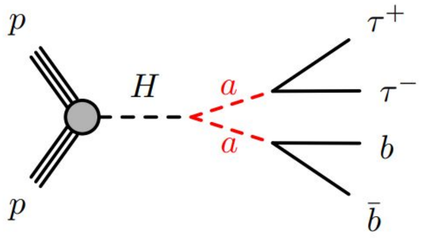

- Run 2 data (140 fb^{-1}), search in 12 < m(a) < 60 GeV.
- **Low mass region:** bb as a single fat jet (B).
- **High mass region:** b-jets are well resolved.
- New algorithm (DeXTer) to classify fat jets by reconstructing SVs in the jet.

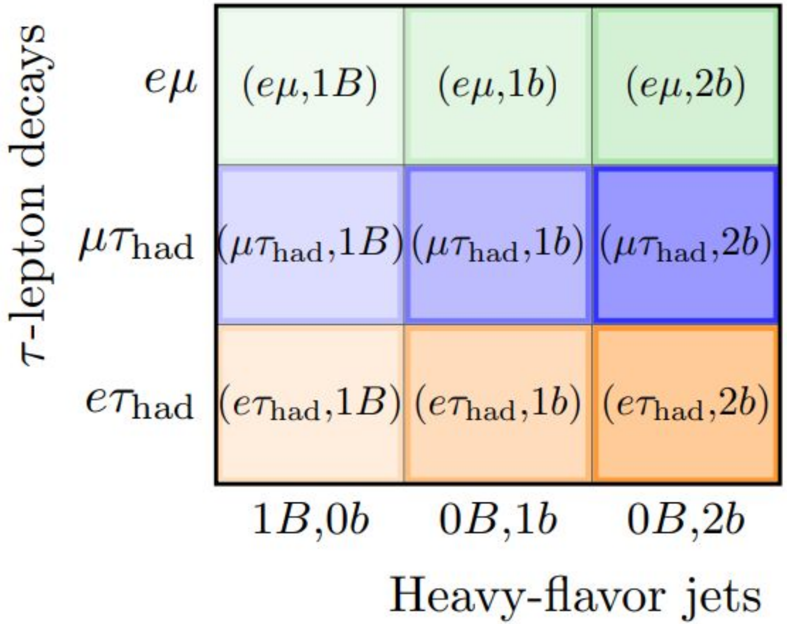

H → aa → 2b2τ [2407.01335]

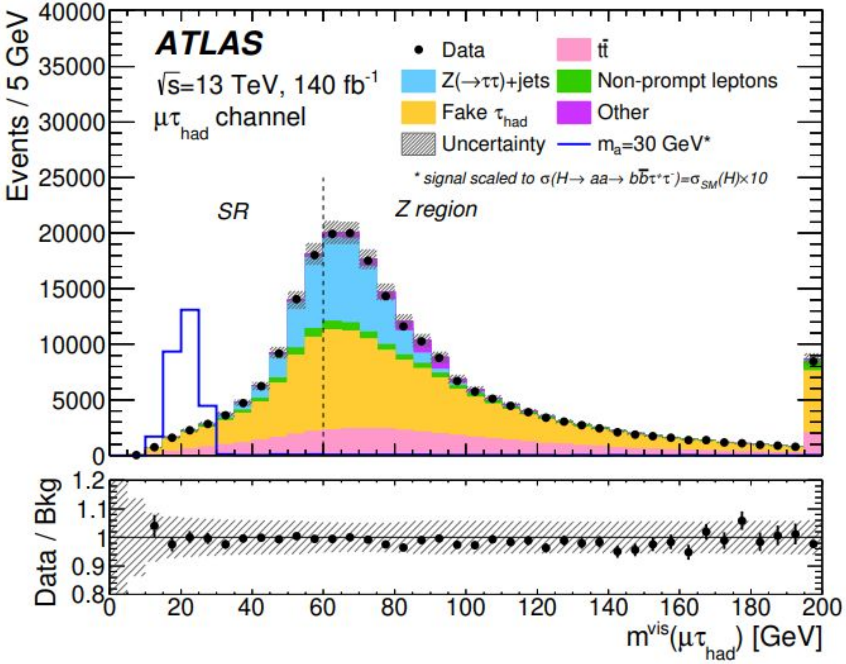

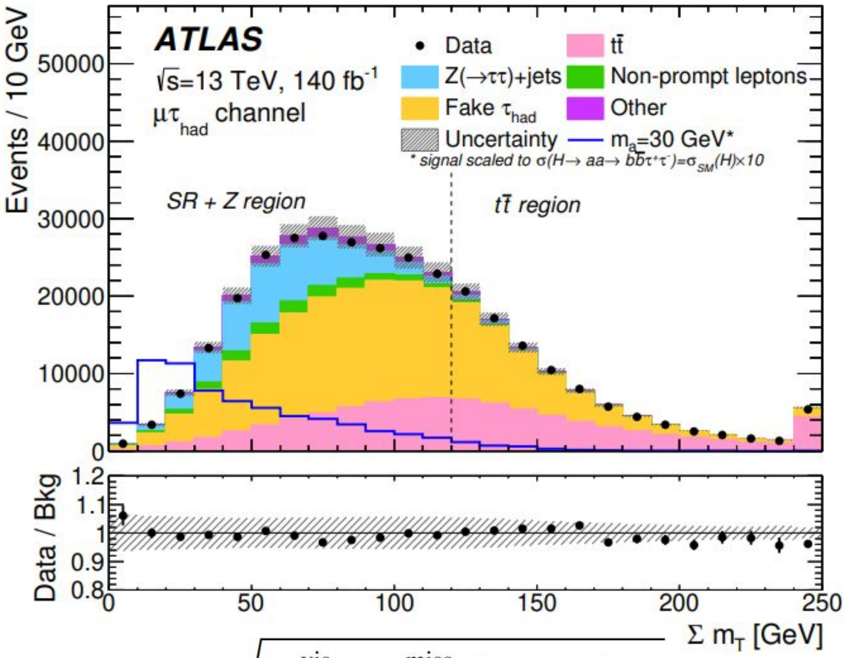

$$m_{\mathrm{T}}(\tau) = \sqrt{2 p_{\mathrm{T}}^{\mathrm{vis}}(\tau) E_{\mathrm{T}}^{\mathrm{miss}} (1 - \cos(\Delta\phi))}.$$

H → aa → 2b2τ [2407.01335]

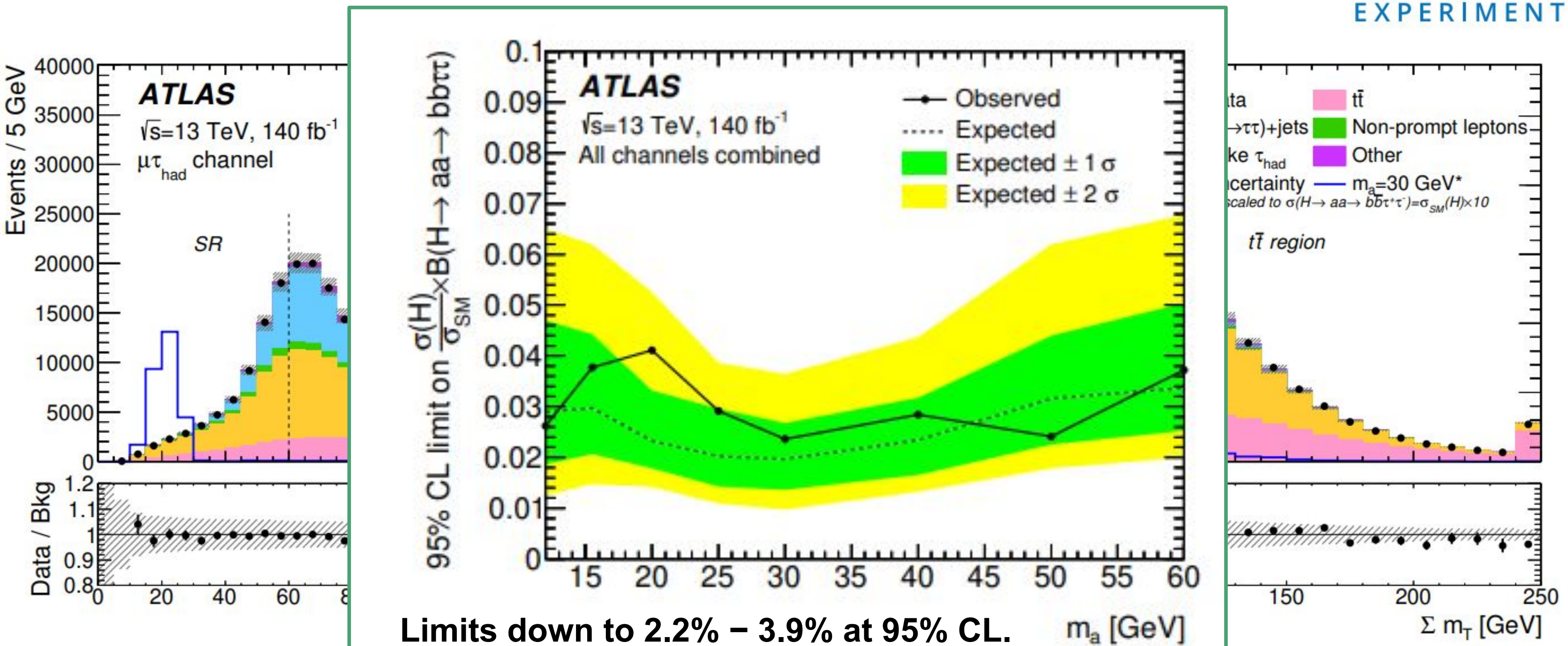

Limits down to 2.2% − 3.9% at 95% CL.

H → aa → 2b2μ/τ [2402.13358]

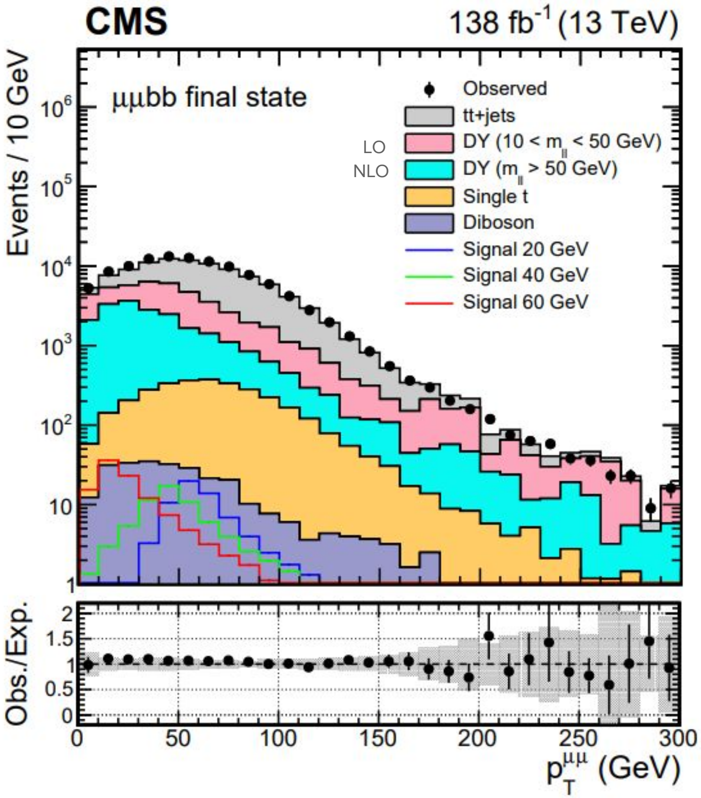

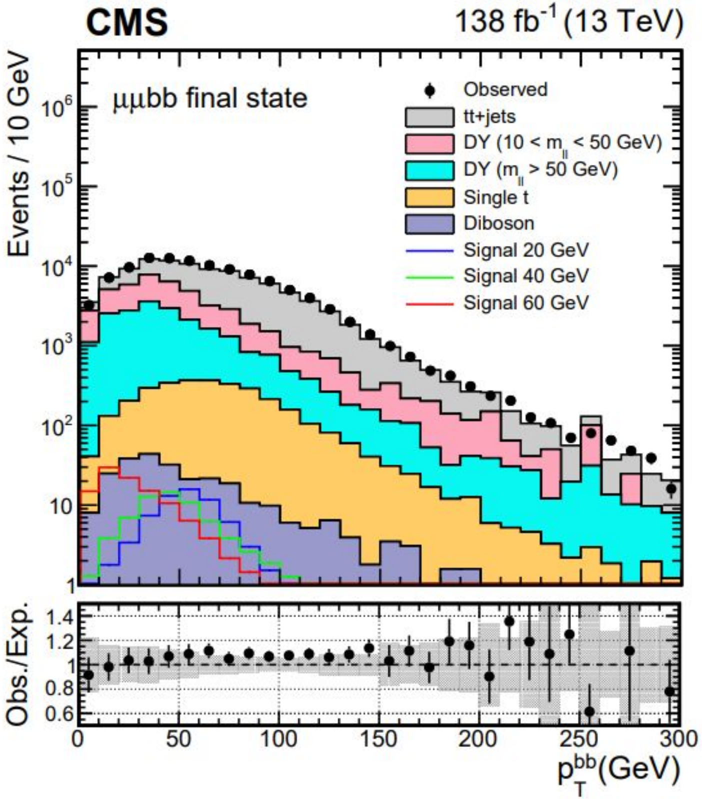

H → aa → 2b2μ/τ [2402.13358]

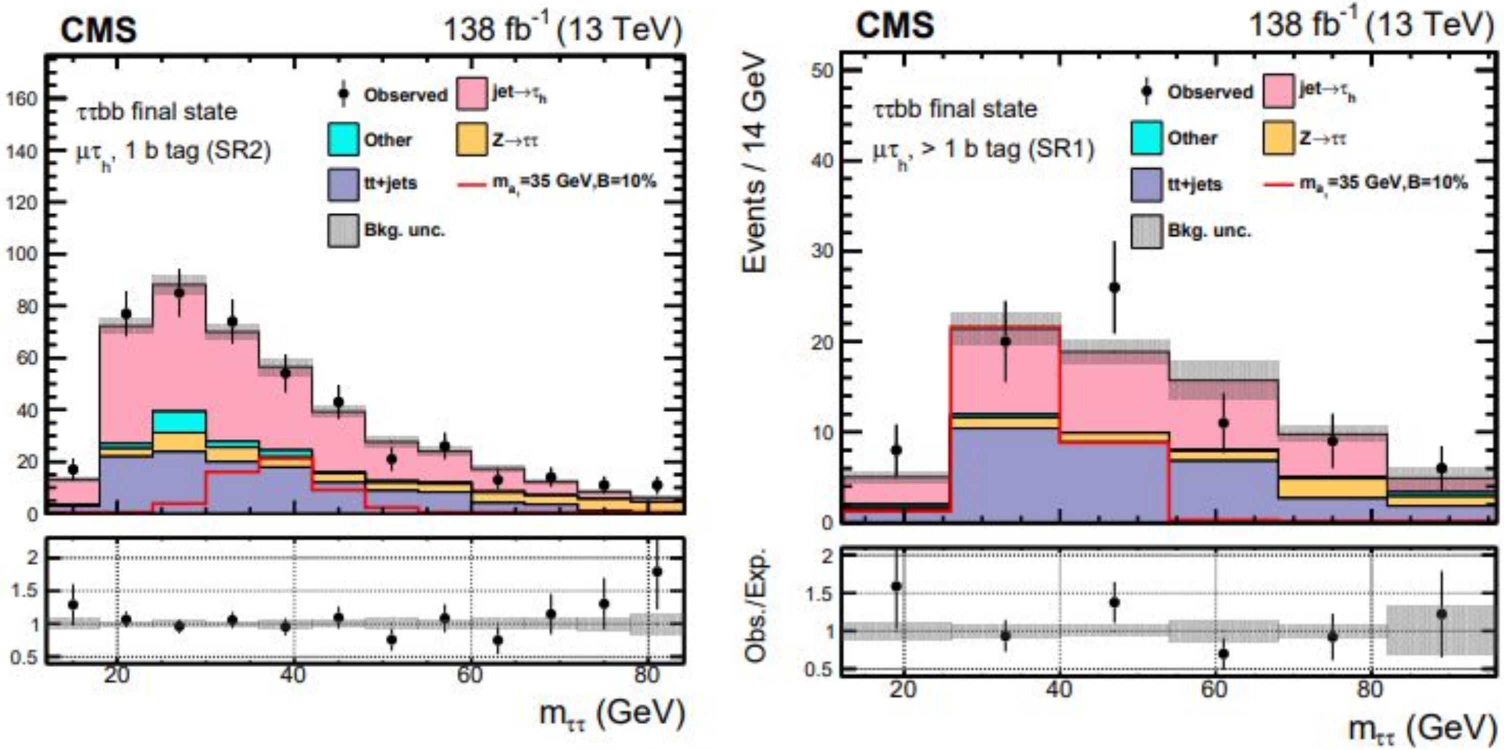

H → aa → 2b2μ/τ [2402.13358]

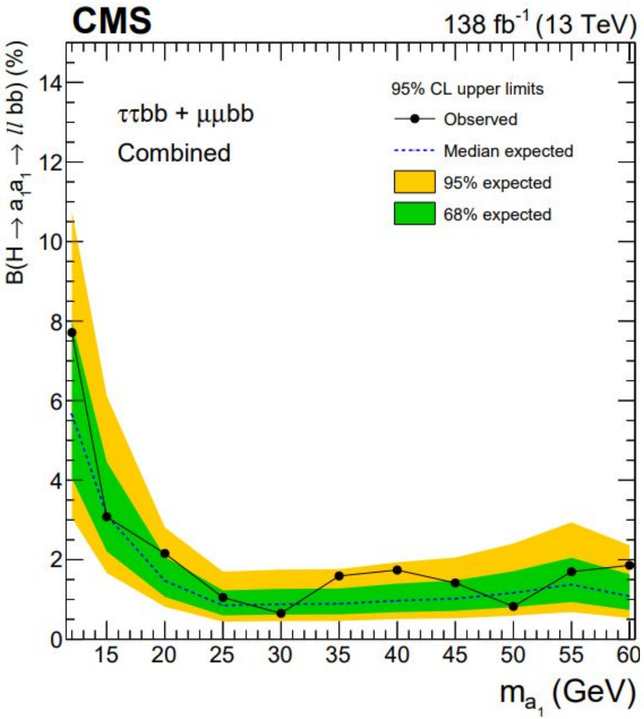

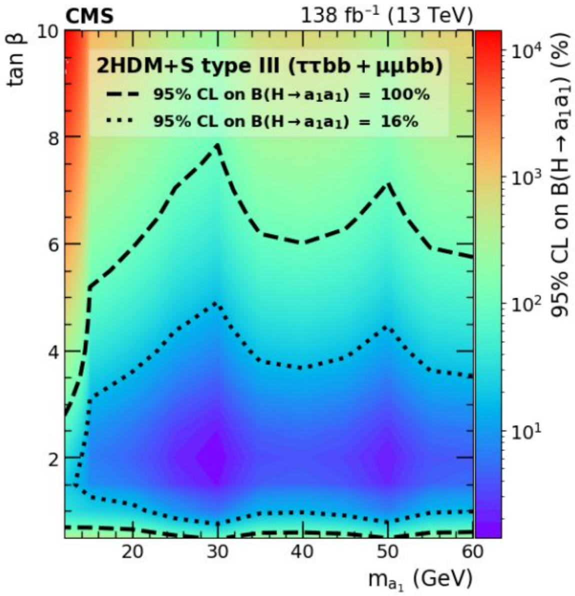

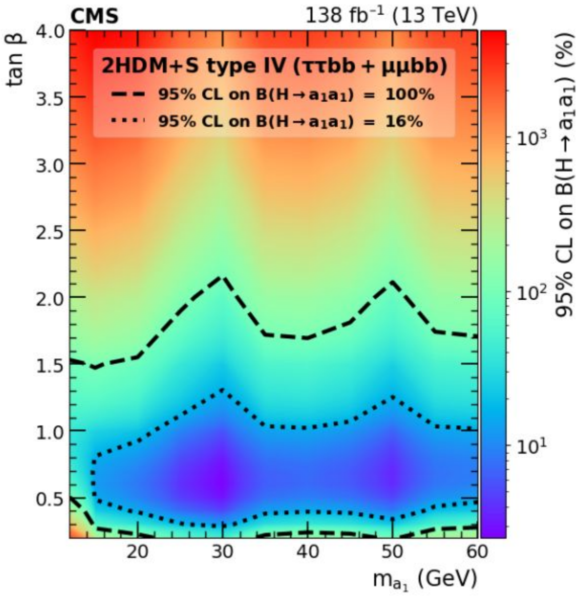

Limits down to 0.6% at 95% C.L.

BR = 16% from 2207.00043 (CMS Run 2 results)

H ➔ aa ➔ 4μ [2407.20425]

- Prompt: 2017+2018+2016
- Displaced: 2017+2018
- Limits provided for various models

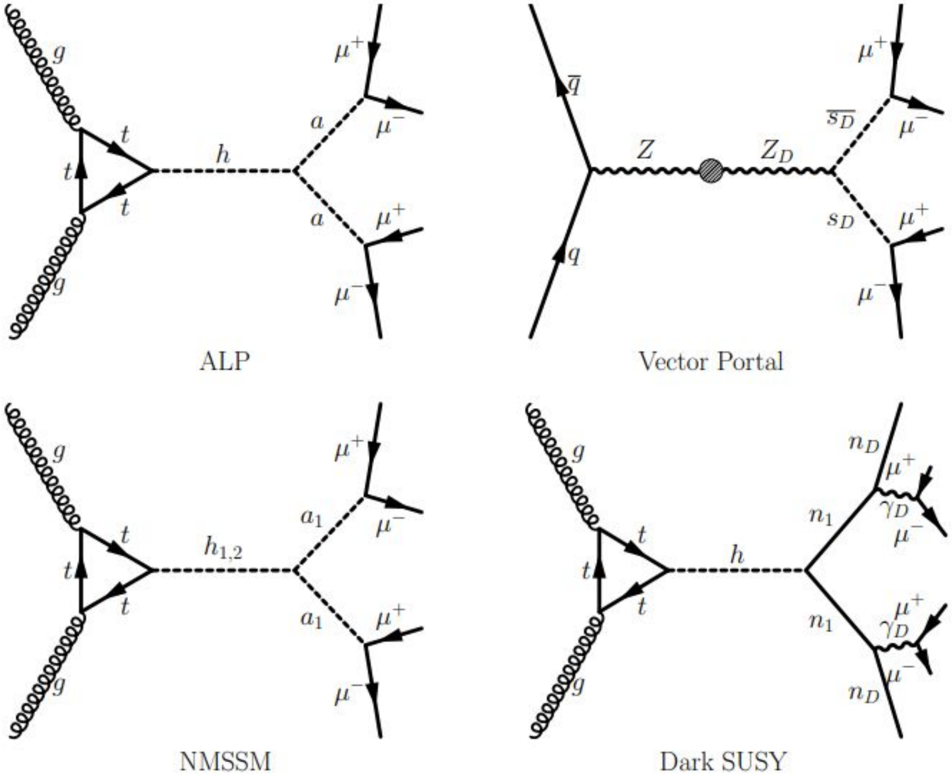

H → aa → 4μ [2407.20425]

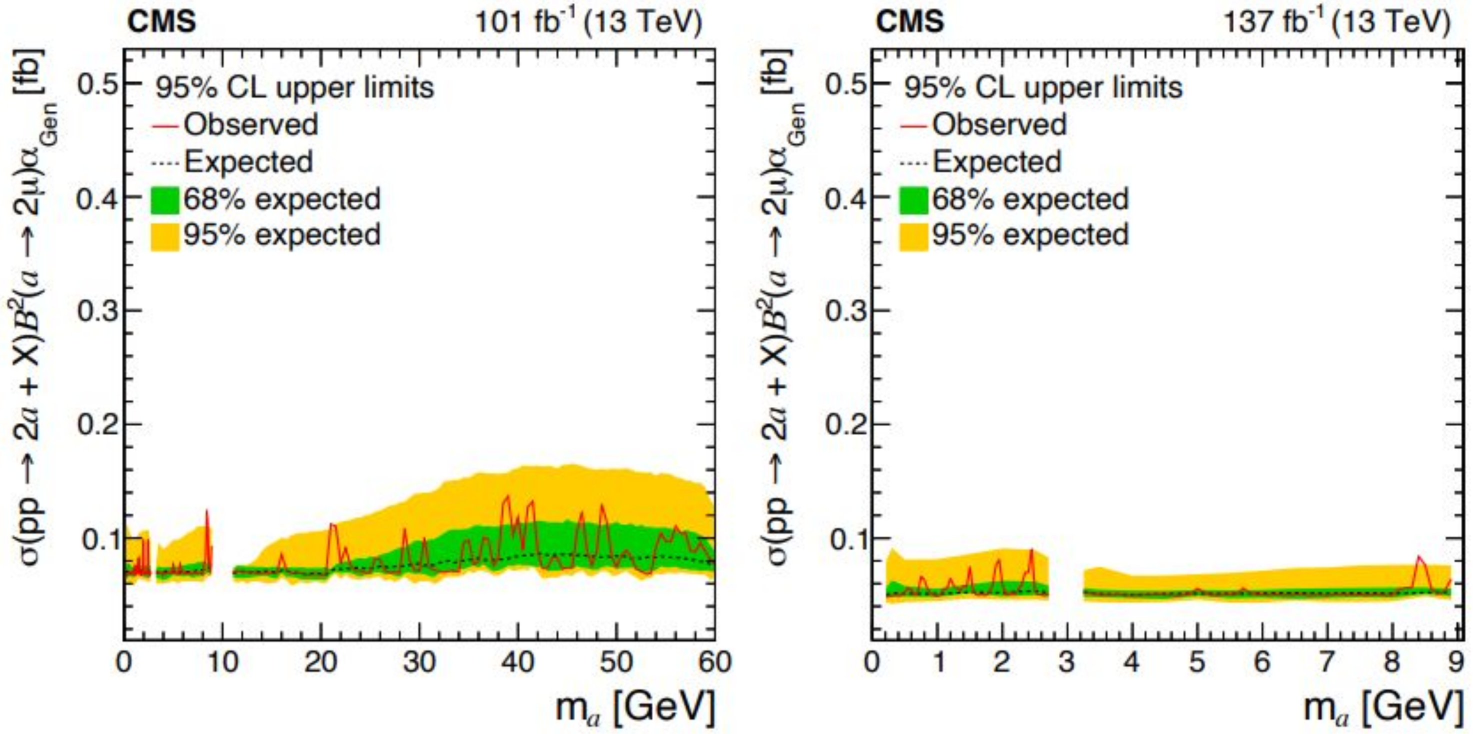

H → aa → 4μ [2407.20425]

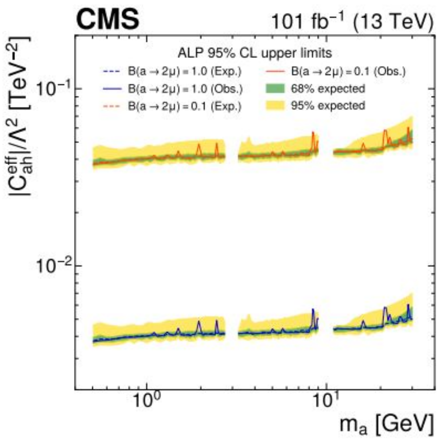

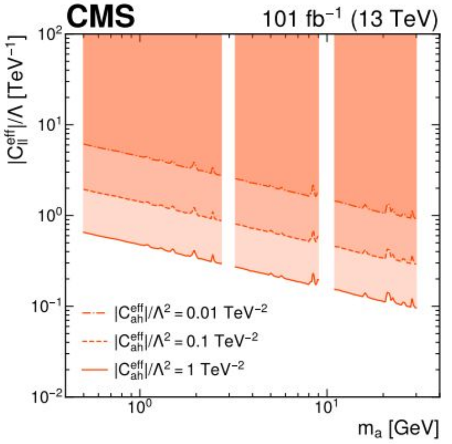

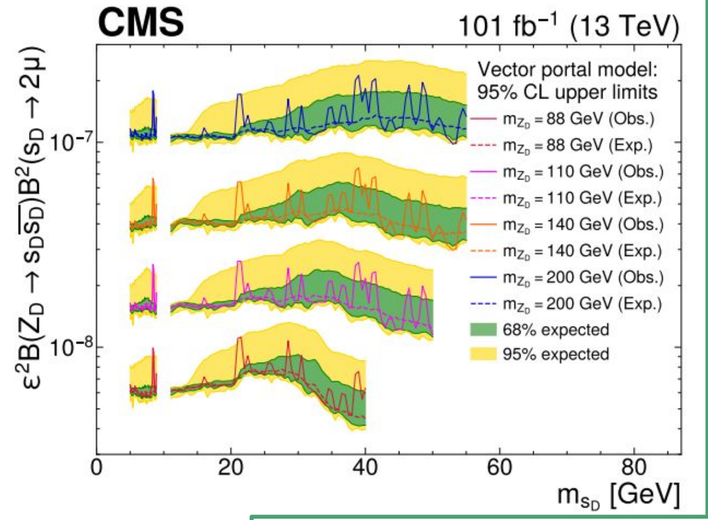

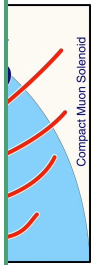

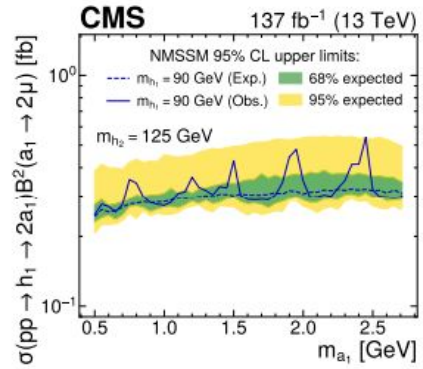

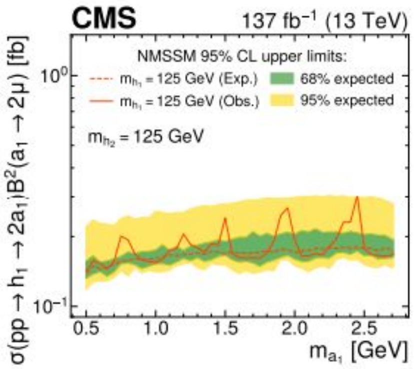

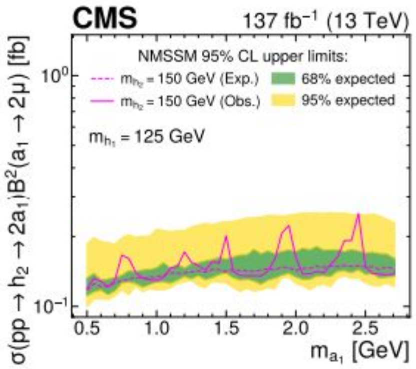

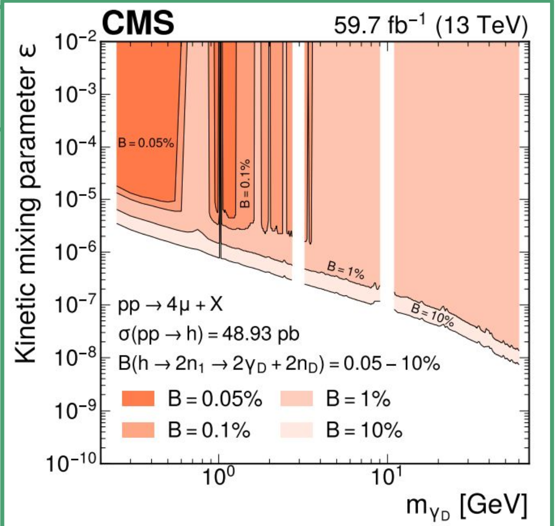

H → aa → 4b [2403.10341]

Higgs in association with V

m(a) = 60 GeV hypothesis in plots

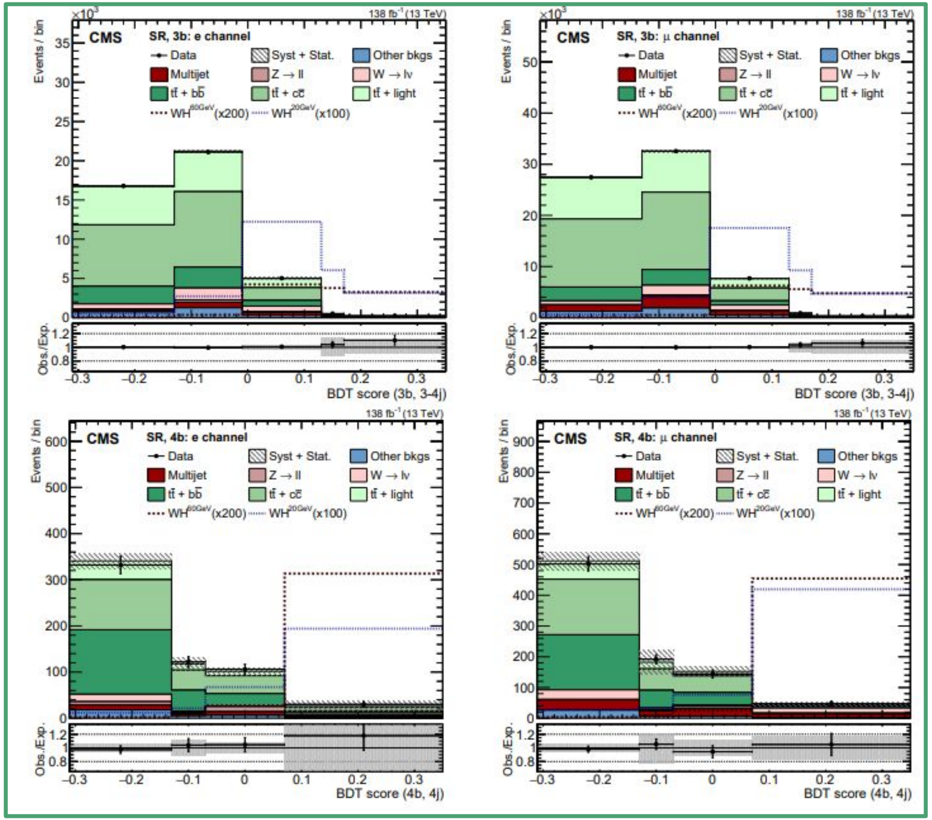

Label	(N_b, N_j)	Description
	WH channel	
SR (3b)	(3b, 3–4j)	3b signal region
SR (4b)	(4b, 4j)	4b signal region
CR (3b)	(2b, 3j)	W / $t\bar{t}$ +jets control region
CR (4b)	(2b, 4j)	$t\bar{t}$ +jets control region
	ZH channel	
SR (3b)	(3b, ≥3j)	3b signal region
SR (4b)	(4b, ≥4j)	4b signal region
CR (3b)	(2b, 3j)	DY control region
CR (4b)	(2b, 4j)	DY control region

$H \to aa \to 4b$ [2403.10341]

Higgs in association with V

m(a) = 60 GeV hypothesis in plots

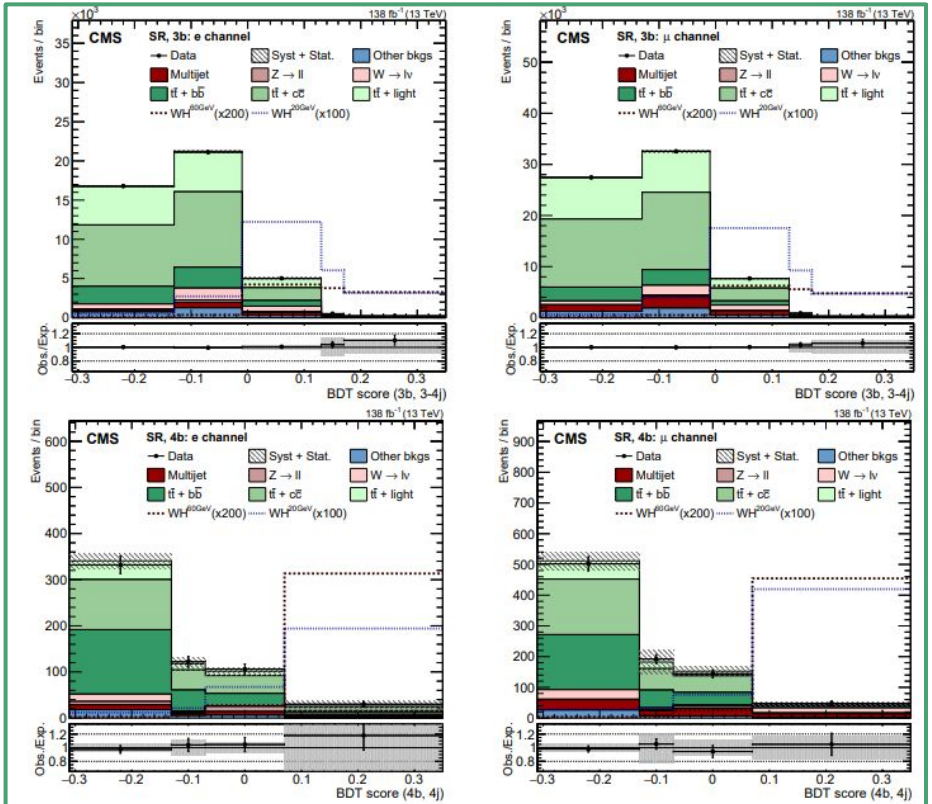

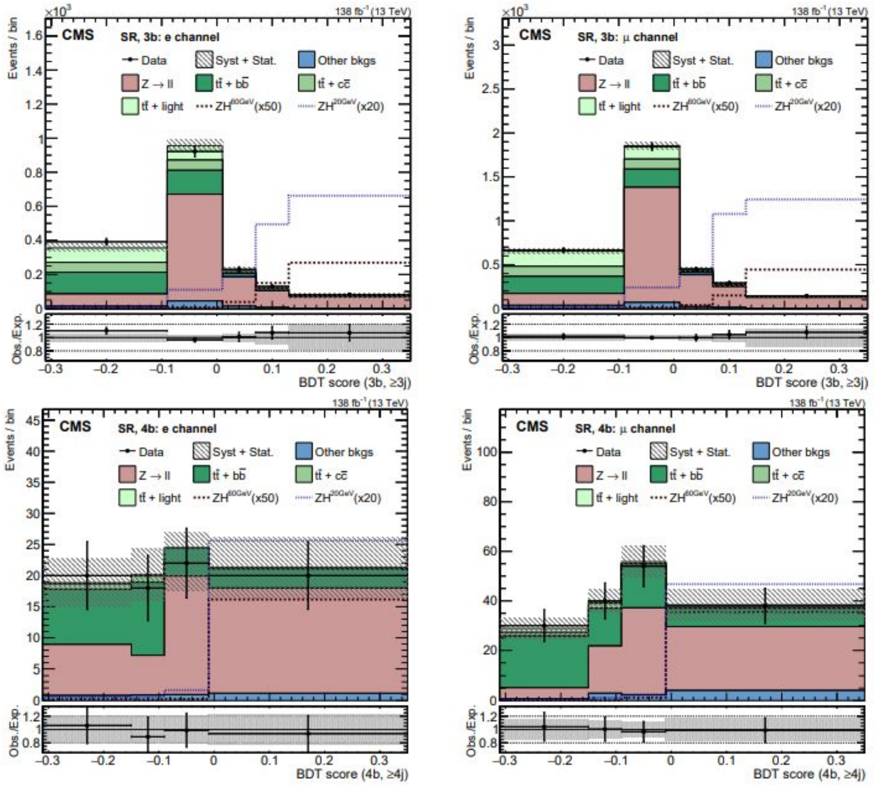

H → aa → 4b

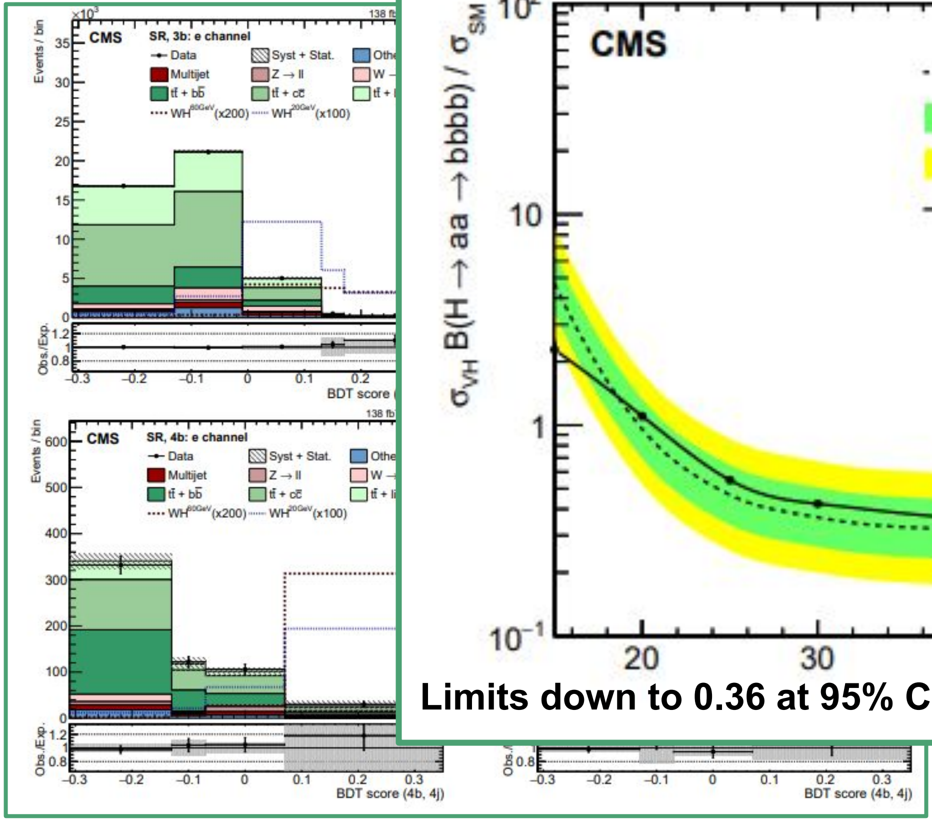

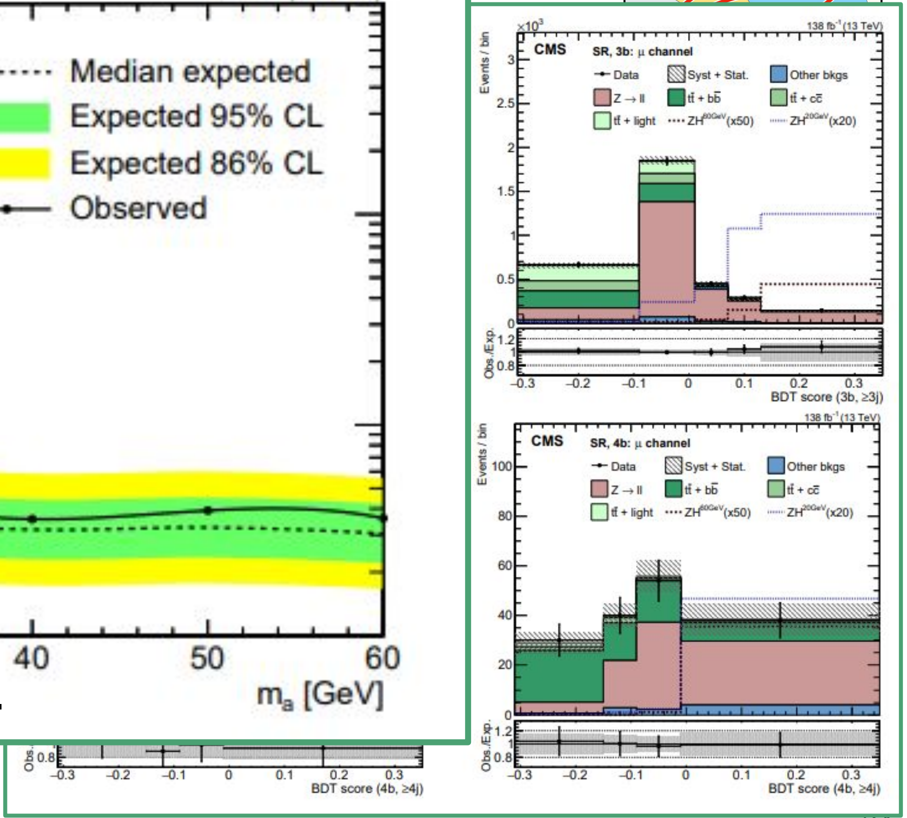

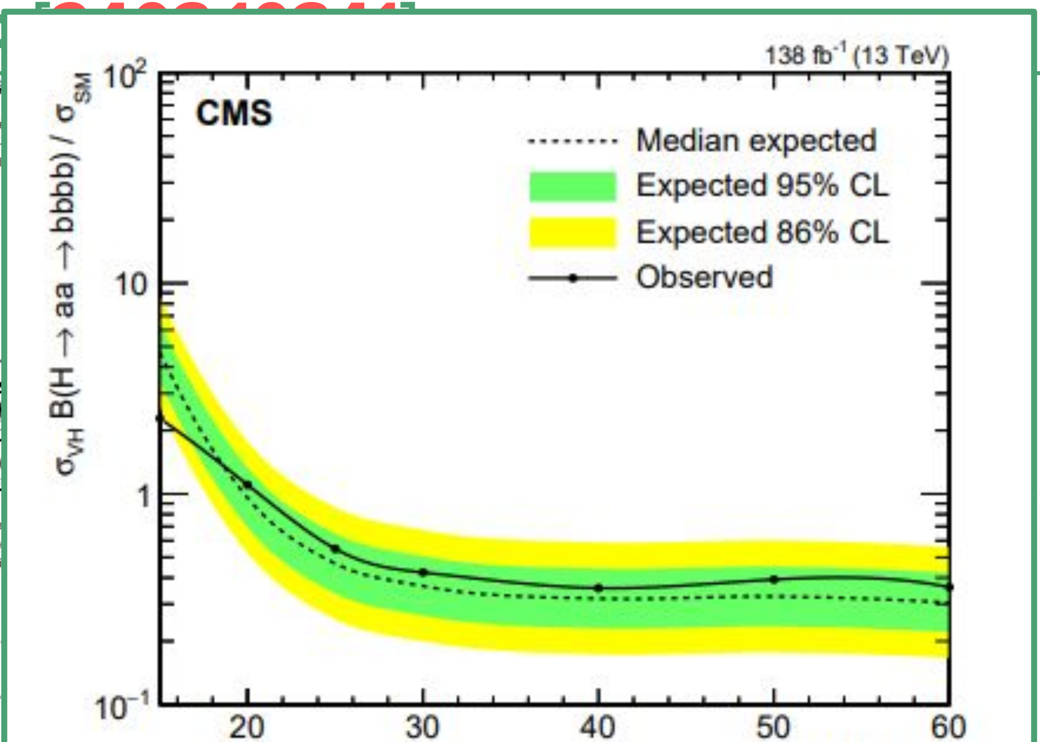

Limits down to 0.36 at 95% CL.

H → aa → 4γ [2312.03306]

Prompt and displaced search

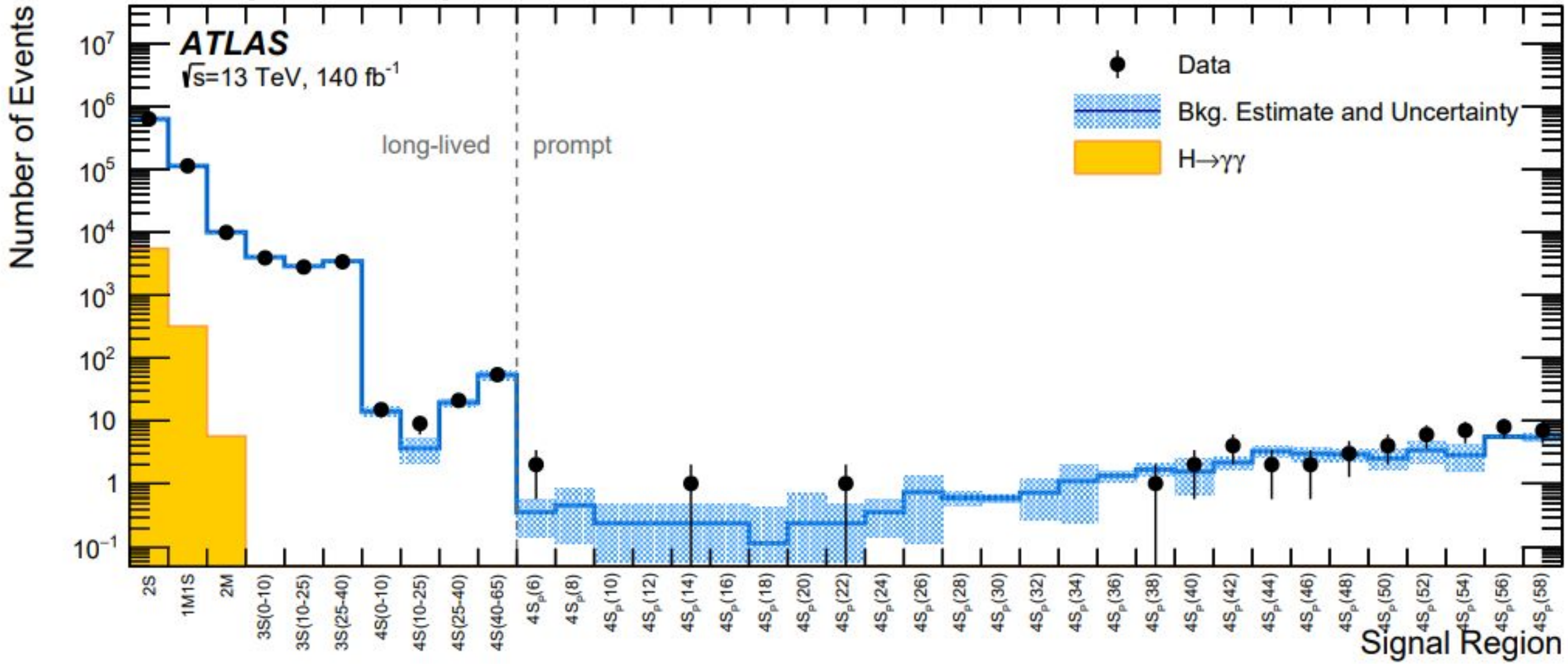

H → aa → 4γ [2312.03306]

$$\Gamma_{a\gamma\gamma} = \frac{4\pi\alpha^2 m_a^3}{\Lambda^2}|C_{a\gamma\gamma}|^2.$$

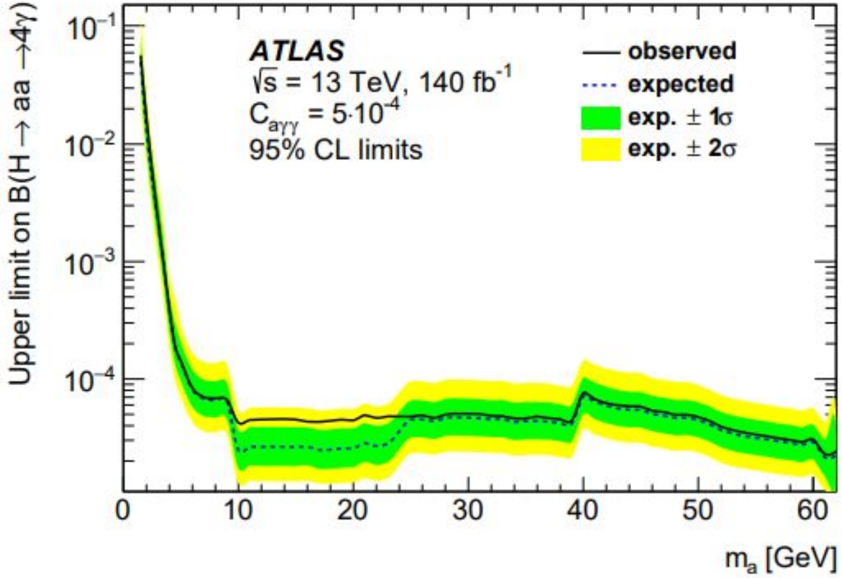

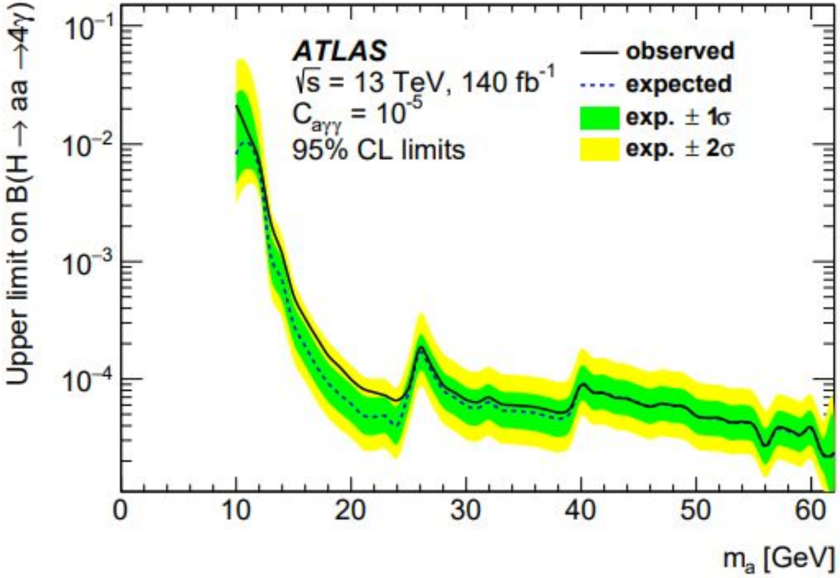

H → aa → 4γ [2312.03306]

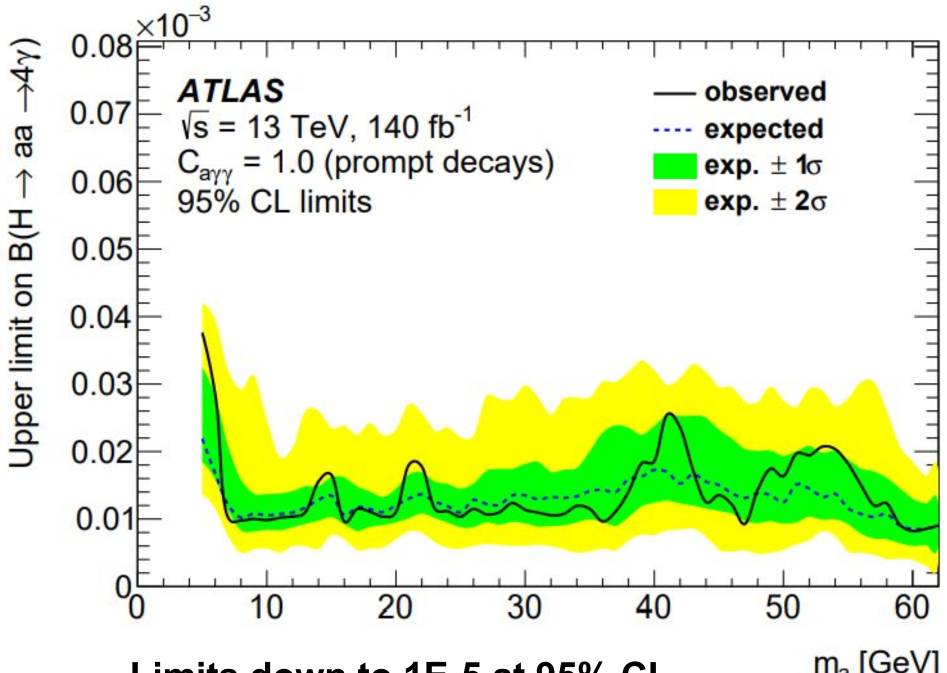

Limits down to 1E-5 at 95% CL.

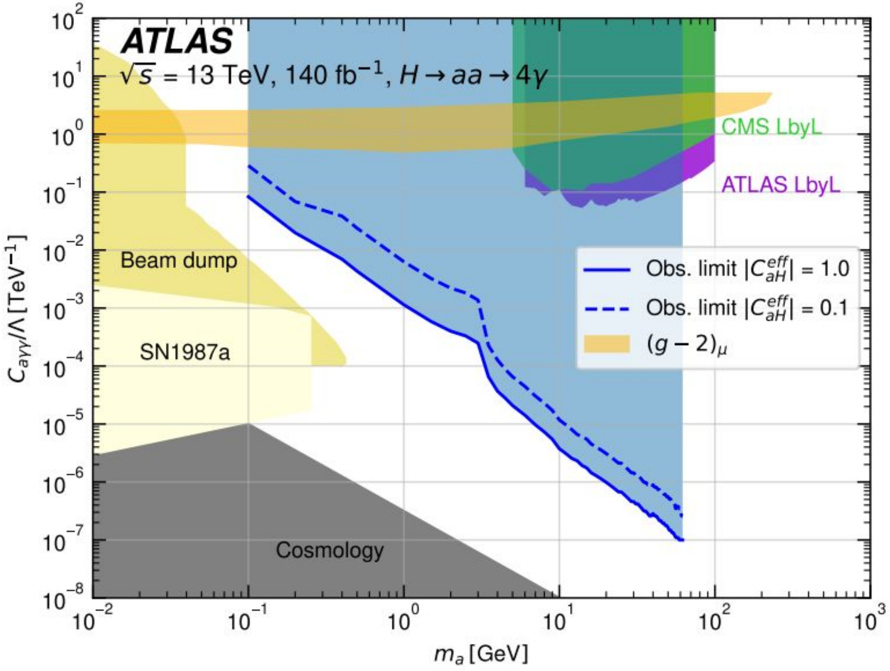

H → χχ (χ → bb) [1705.07332]

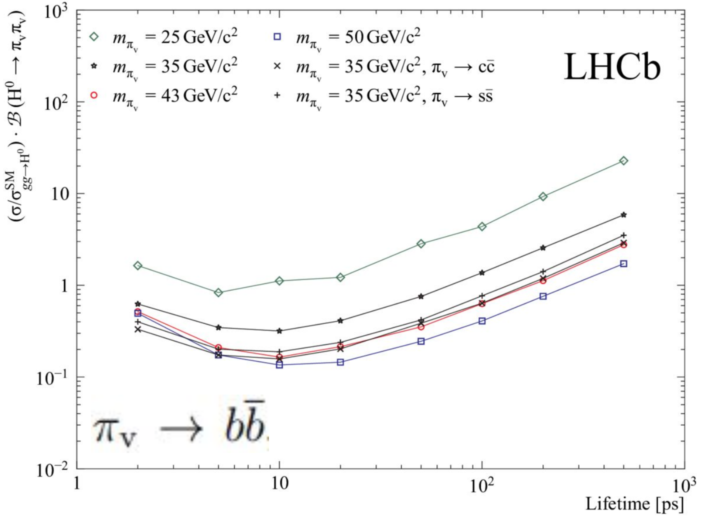

H → χχ (χ → eμν) [2012.02696]

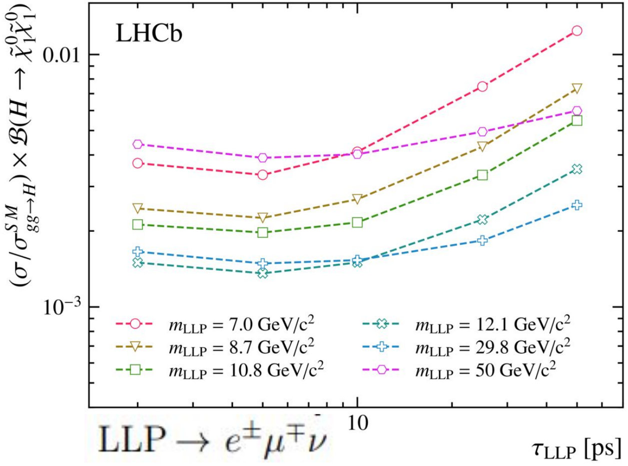

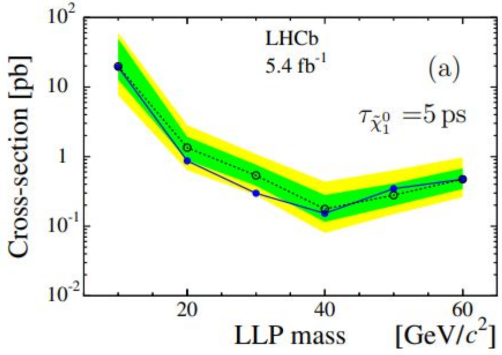

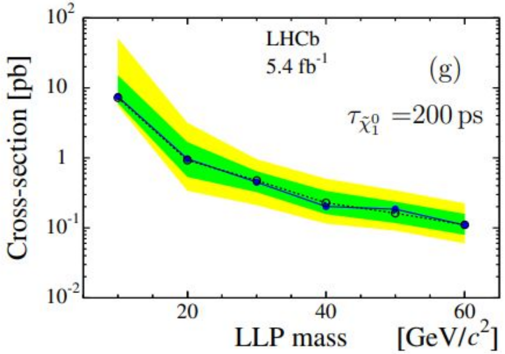

H → χχ (χ → μ2q) [2110.07293]

$$\tilde{\chi}^0_1 \to \mu^+ q_i q_j (\mu^- \bar{q}_i \bar{q}_j)$$

H → Za (a→2γ) [2312.01942]

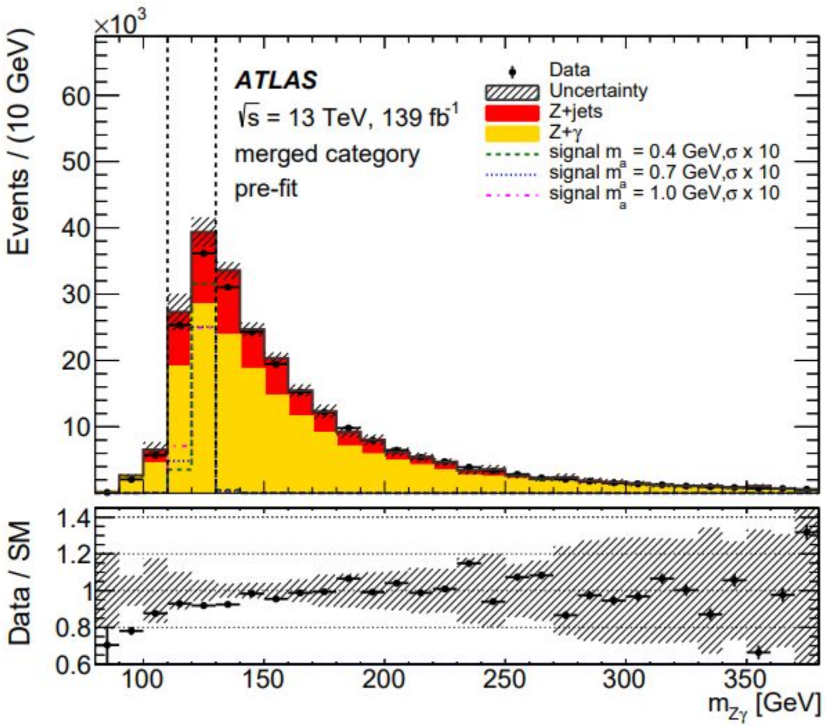

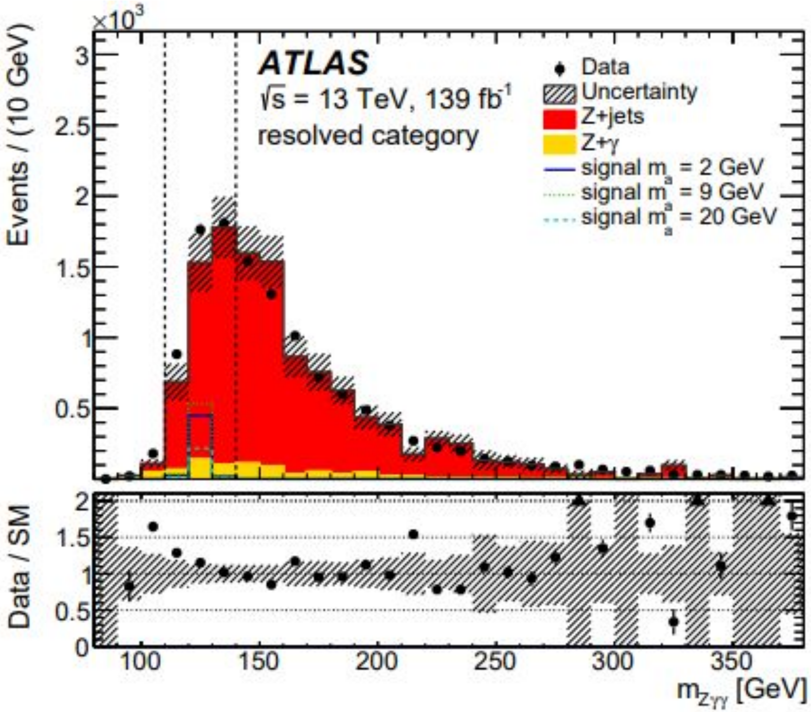

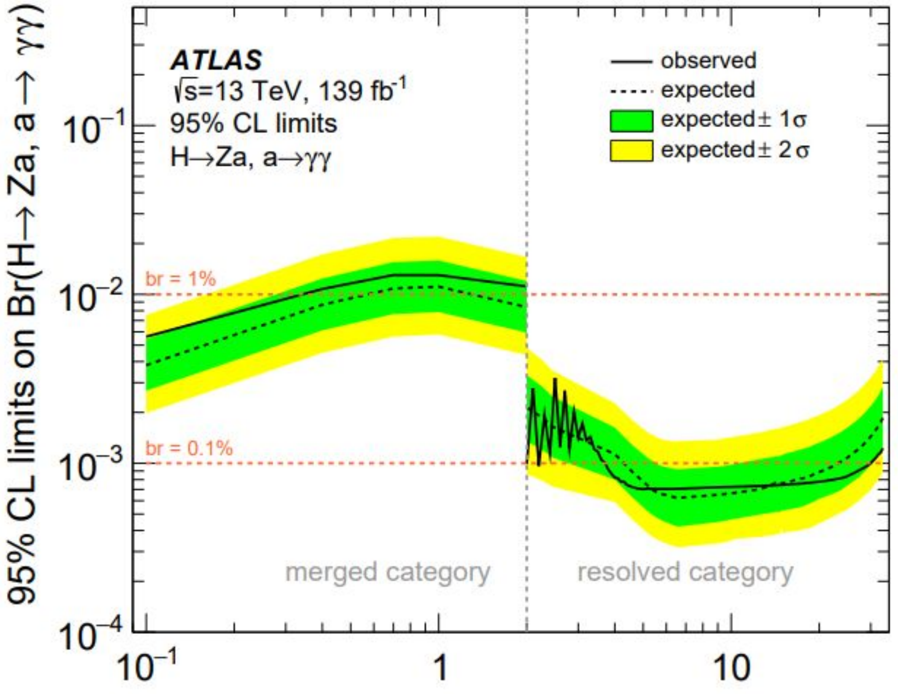

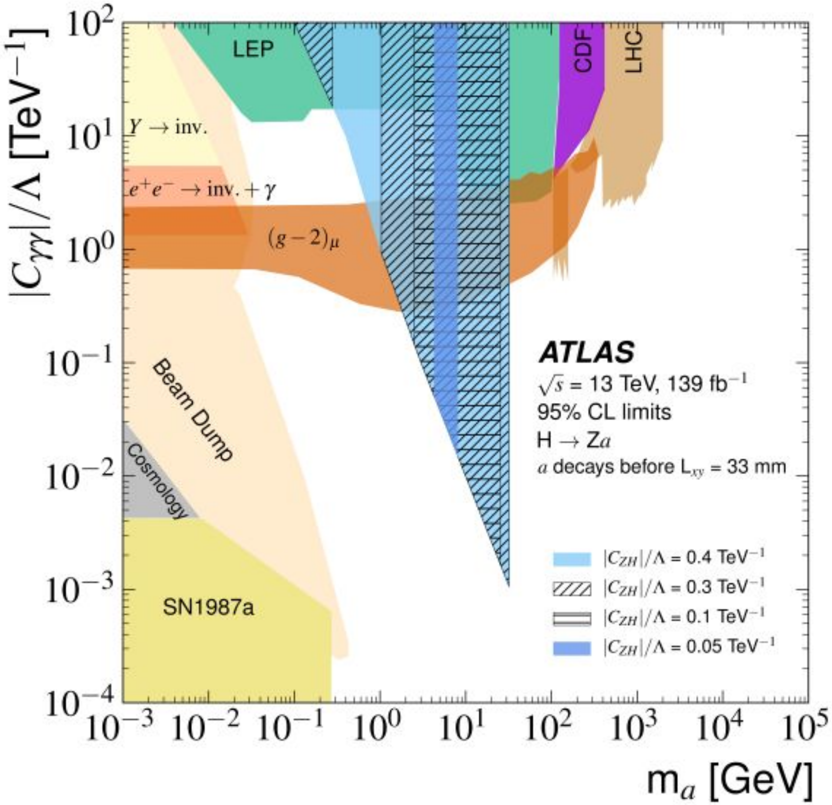

Limits down to 0.08% at 95% CL.

Prospects with LHCb MS

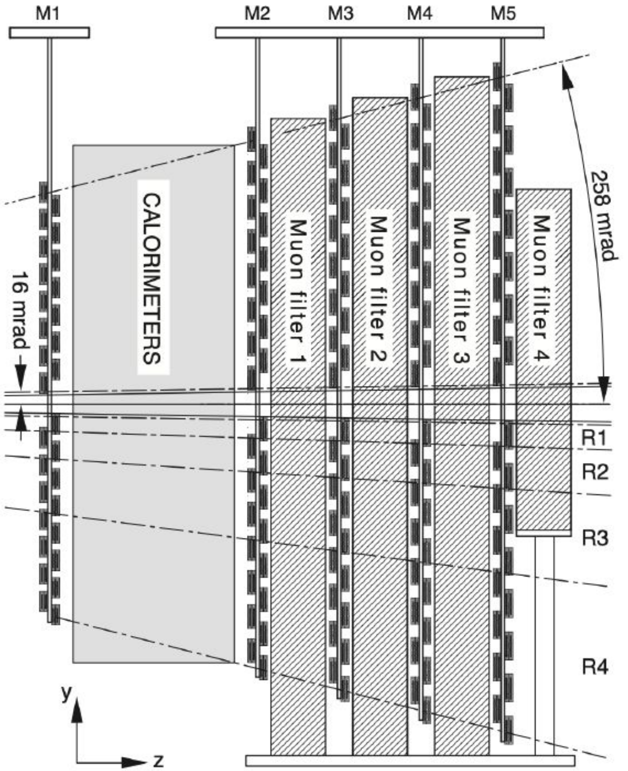

LHCb-TDR-4

Prospects with LHCb MS

[LHCb-FIGURE-2024-015]

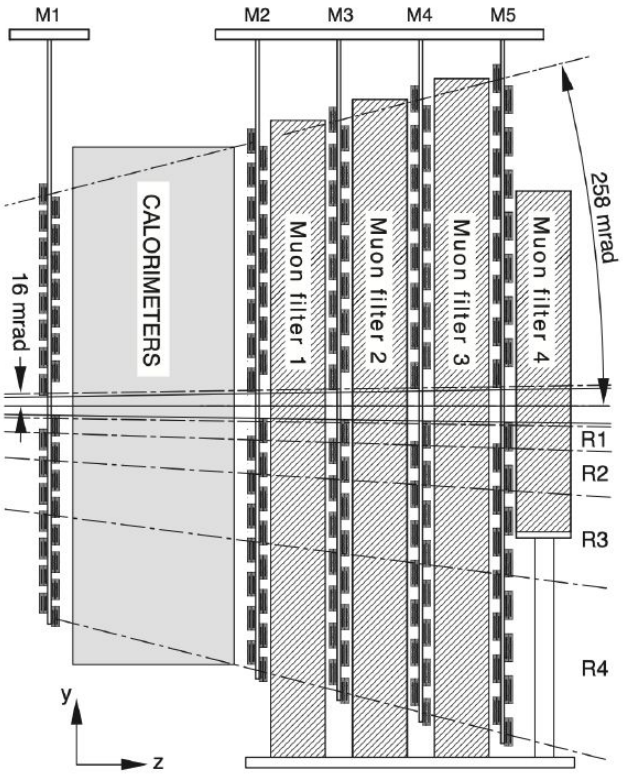

[LHCb-TDR-4]

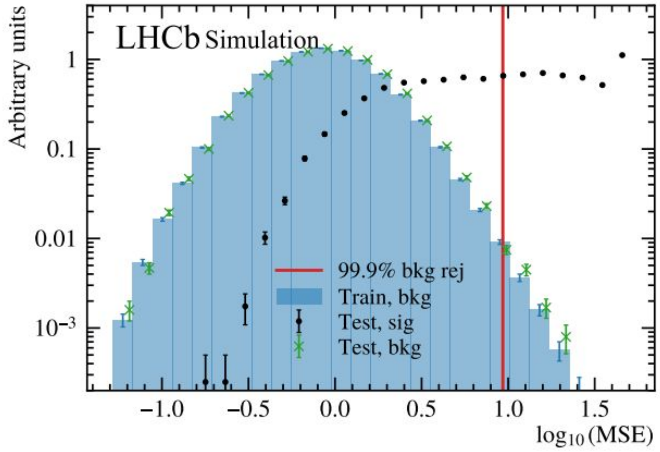

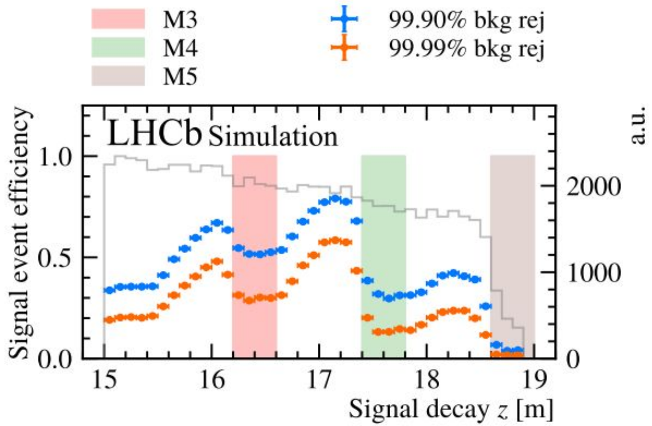

Intermezzo

CODEX-b

FASER

ANUBIS

THE MILLIQAN sub-detector

SHiP

Search for Hidden Particles

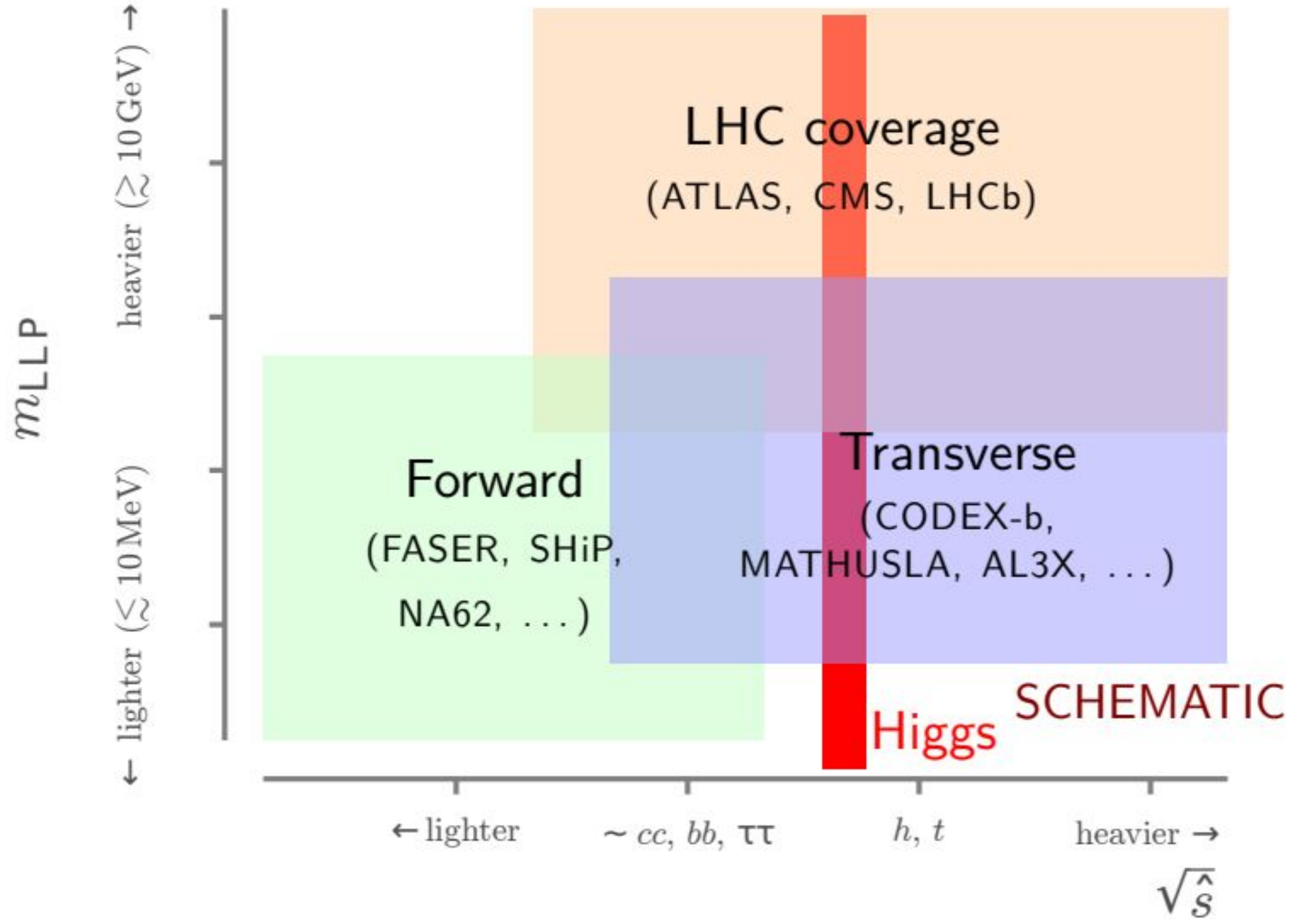

LHC coverage
(ATLAS, CMS, LHCb)
Forward
(FASER, SHiP, NA62, ...)
Transverse
(CODEX-b, MATHUSLA, AL3X, ...)
Higgs
SCHEMATIC
m_{LLP}
heavier ($\gtrsim$ 10 GeV) →
← lighter ($\lesssim$ 10 MeV)
← lighter
$\sim cc,\ bb,\ \tau\tau$
$h,\ t$
heavier →
$\sqrt{\hat{s}}$

Higgs to invisible (HL-LHC) limit
arXiv:1902.00134

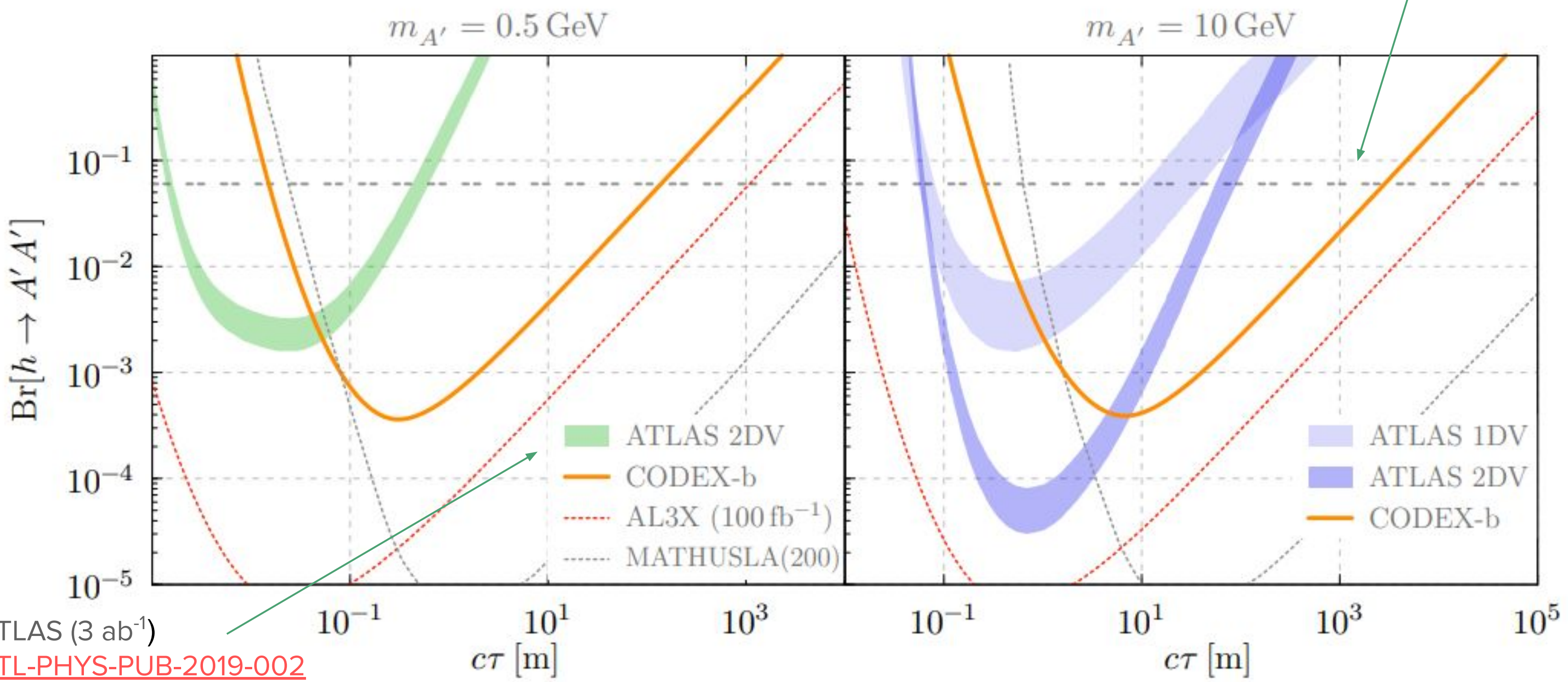

ATLAS (3 ab^{-1})
ATL-PHYS-PUB-2019-002
Phys. Rev. D 99, 052005

Summary

Exotic Higgs decays are a natural and expected signature for BSM.

We should keep the good pace ➔ keep searching.

SM measurements are also crucial ➔ keep constraining.

Not only in the ATLAS, CMS and LHCb ➔ **dedicated detectors, future colliders.**

Summary

Exotic Higgs decay

We should keep th

SM measurement

Not only in the ATL **olliders.**

Thanks.

Backup.

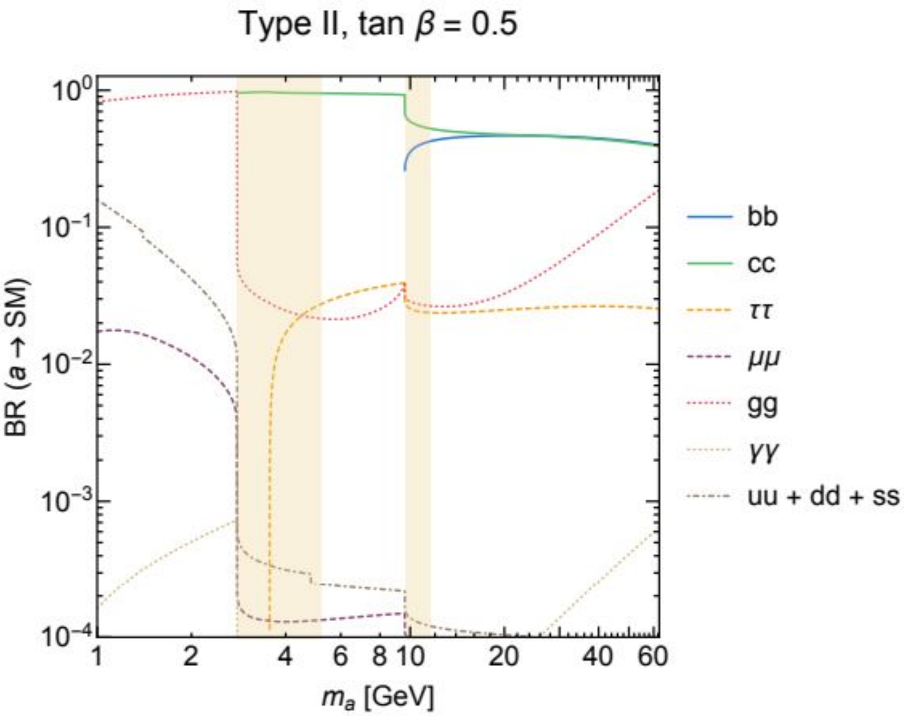
Type II, tan β = 0.5
BR (a → SM)
m_a [GeV]
bb
cc
ττ
μμ
gg
γγ
uu + dd + ss

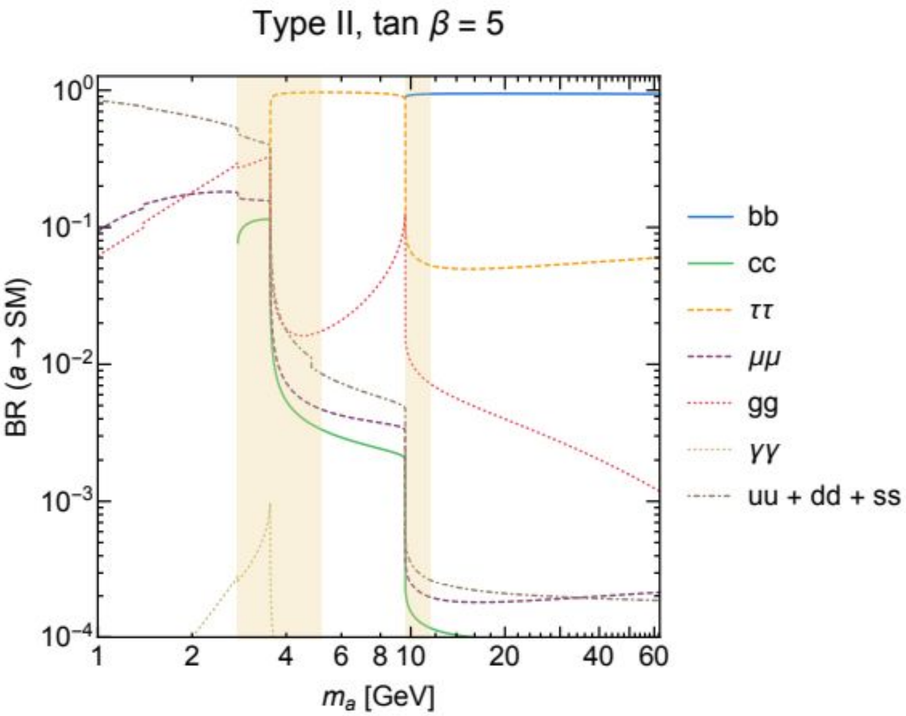
Type II, tan β = 5
BR (a → SM)
m_a [GeV]
bb
cc
ττ
μμ
gg
γγ
uu + dd + ss

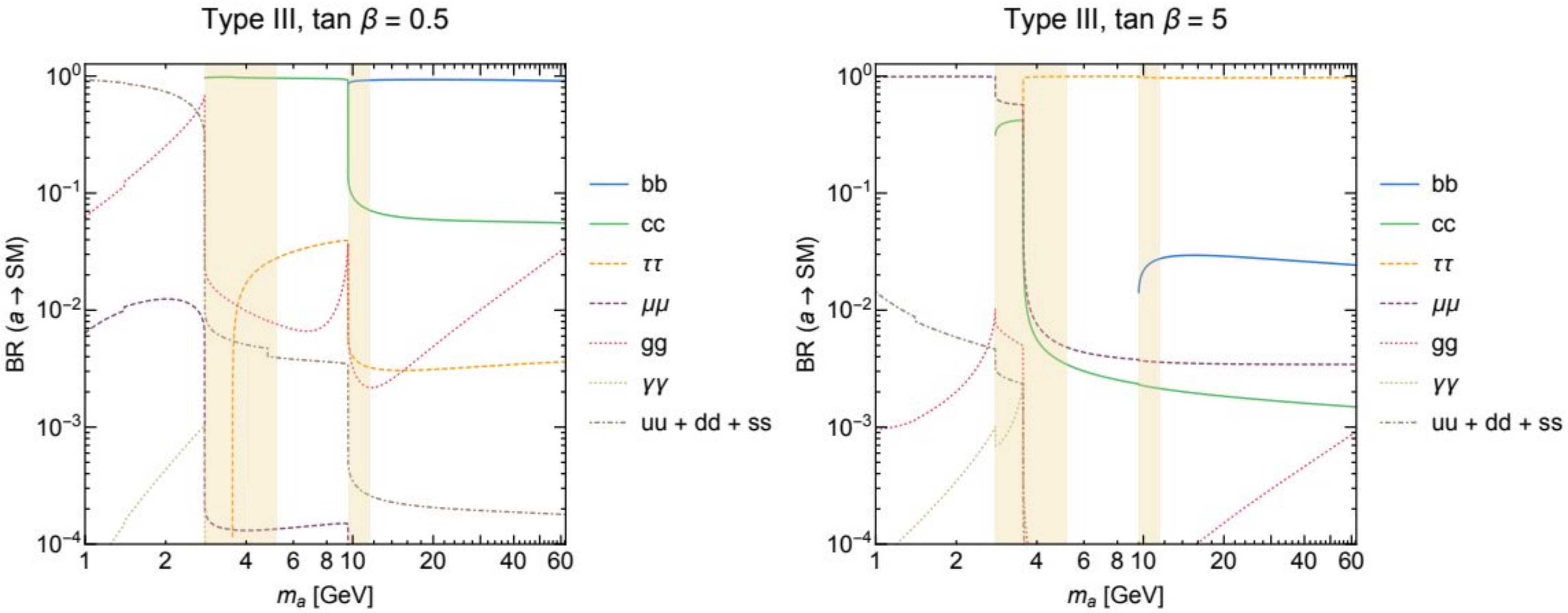
Type III, tan β = 0.5
Type III, tan β = 5
BR (a → SM)
m_a [GeV]
bb
cc
ττ
μμ
gg
γγ
uu + dd + ss

H → aa → 2b2τ [2407.01335]

Region	$e\mu$	$e\tau_{\text{had}}$ or $\mu\tau_{\text{had}}$
Signal region	1 OS signal $e\mu$ pair 0 signal τ_{had} $\Delta R(e,\mu) > 0.1$ $4 < m^{\text{vis}}(\tau\tau) < 45$ GeV	1 OS signal $e\tau_{\text{had}}$ or $\mu\tau_{\text{had}}$ pair 1 signal τ_{had} $\Delta R(\ell,\tau) > 0.2$ $4 < m^{\text{vis}}(\tau\tau) < 60$ GeV
	$\Sigma m_T < 120$ GeV 1 B-jet or 1 or 2 b-jets	
Z region	$m^{\text{vis}}(\tau\tau) > 45$ GeV	$m^{\text{vis}}(\tau\tau) > 60$ GeV
$t\bar{t}$ region	$\Sigma m_T > 120$ GeV, no $m^{\text{vis}}(\tau\tau)$ requirement	
SS region	1 SS signal $e\mu$ pair	1 SS signal $e\tau_{\text{had}}$ or $\mu\tau_{\text{had}}$ pair

H → aa → 2b2τ [2407.01335]

pNN = parametrised NN

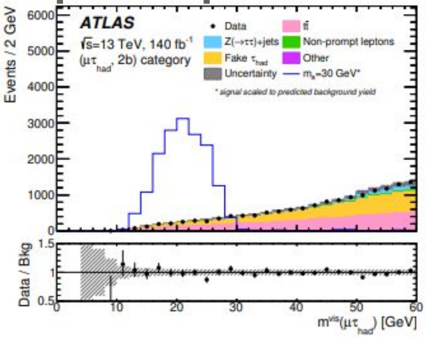

(a)

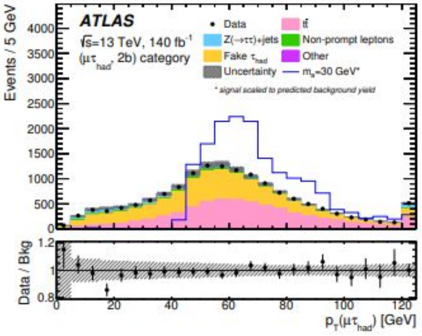

(b)

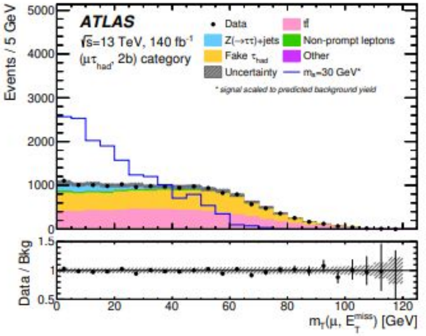

(c)

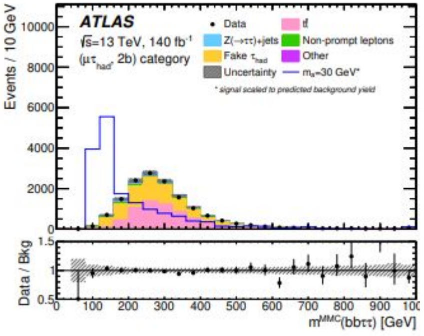

(d)

Table 2: Neural-network input variables with a summary of the final-state property it describes.

Feature	Description
$m^{\text{true}}(\tau\tau)$	During training: generated a-boson mass for signal MC. Background events are assigned a random value of the eight signal masses. During testing: the mass hypothesis under consideration.
$m^{\text{vis}}(\tau\tau)$	Visible mass of the $\tau\tau$ system.
$p_{\text{T}}(\tau\tau)$	p_{T} of the $\tau\tau$ system.
$m^{\text{MMC}}(\nu\nu)$	MMC-based mass of the two neutrinos in $\tau \to e\nu_\tau\bar{\nu}_e$ or $\tau \to e\nu_\tau\bar{\nu}_\mu$ decays.
$E_{\text{T}}^{\text{miss}}$	Missing transverse energy.
$m_{\text{T}}(\tau)$	Transverse mass calculated with the visible p_{T} of the final-state τ-leptons.
$p_{\text{T}}(b^{\text{lead}})$	Transverse momentum of the leading final-state b-jet.
$p_{\text{T}}^{\text{vis}}(\tau\tau b^{\text{lead}})$	Visible p_{T} of the $\tau\tau b^{\text{lead}}$ system.
D_ζ	Misalignment between the $\vec{E}_T^{\text{miss}}$ vector and the $\tau\tau$ system.
Categories with a B-jet or 2 b-jets	
$p_{\text{T}}(b^{\text{sublead}})$	Transverse momentum of the subleading final-state b-jet.
$p_{\text{T}}(bb)$	Transverse momentum of the bb system.
$m(bb)$	Mass of the bb system.
$m^{\text{vis}}(bb\tau\tau)$	Visible mass of the Higgs boson system.
$m^{\text{MMC}}(bb\tau\tau)$	MMC-based mass of the Higgs boson system.

CR, SR1, SR2 to increase S/B

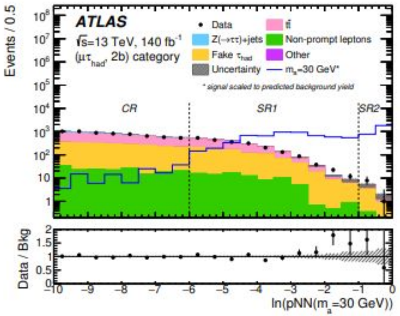

(a)

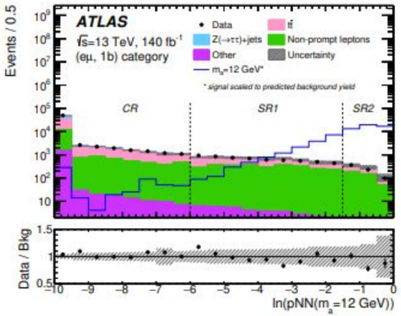

(b)

H → aa → 2b2τ [2407.01335]

Feature
$m^{\text{true}}(\tau\tau)$
$m^{\text{vis}}(\tau\tau)$
$p_{\text{T}}(\tau\tau)$
$m^{\text{MMC}}(\nu$
$E_{\text{T}}^{\text{miss}}$
$m_{\text{T}}(\tau)$
$p_{\text{T}}(b^{\text{lead}})$
$p_{\text{T}}^{\text{vis}}(\tau\tau b^{\text{l}}$
D_{ζ}
$p_{\text{T}}(b^{\text{suble}}$
$p_{\text{T}}(bb)$
$m(bb)$
$m^{\text{vis}}(bb\tau$
$m^{\text{MMC}}(b$

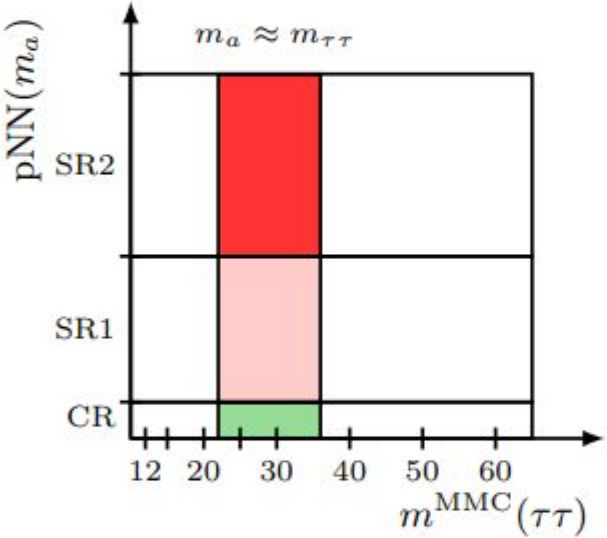

Statistical analysis in nine categories

$$L(\mu,\vec{\alpha}) = \prod_{c}^{N_{\text{cat}}} \prod_{j=1}^{3} \frac{(\mu s_{c,j}(\vec{\alpha}) + b_{c,j}(\vec{\alpha}))^{n_{c,j}}}{n_{c,j}!} e^{-(\mu s_{c,j}(\vec{\alpha})+b_{c,j}(\vec{\alpha}))} \prod_{k=1}^{N_{\text{syst}}} \frac{1}{\sqrt{2\pi}} e^{-\frac{\alpha_k^2}{2}},$$

where μ is the signal strength, $\vec{\alpha}$ is the vector of nuisance parameters, $s_{c,j}$ and $b_{c,j}$ are the expected number of signal and background events in the j^{th} bin of the category c, and $n_{c,j}$ is the observed number of events. Since the signal templates are normalized to the SM Higgs inclusive cross section, the signal strength is equal to $(\sigma(H)/\sigma_{\text{SM}}(H))\mathcal{B}(H \to aa \to b\bar{b}\tau^+\tau^-)$. Note that the values $s_{c,j}$ and $b_{c,j}$ are themselves functions of the set of NPs. Each systematic uncertainty is fully correlated across all bins and categories.

H → aa → 2b2μ/τ [2402.13358]

Table 1: The electron, muon, and τ_h p_T thresholds in GeV at trigger level for the $\mu\mu$bb and $\tau\tau$bb channels.

Year	Single/dilepton trigger p_T	$\mu\mu$bb	$\tau\tau$bb					
			eμ		eτ_h		$\mu\tau_h$	
		μ	e	μ	e	τ_h	μ	τ_h
2016	Single lepton	24	—	—	25	—	22	—
	p_T-leading lepton	17	23	23	—	—	—	20
	p_T-subleading lepton	8	12	8			19	—
2017	Single lepton	24	—	—	27, 32	—	24, 27	—
	p_T-leading lepton	17	23	23	—	30	—	27
	p_T-subleading lepton	8	12	8	24	—	20	—
2018	Single lepton	24	—	—	32, 35	—	24, 27	—
	p_T-leading lepton	17	23	23	—	30	—	27
	p_T-subleading lepton	8	12	8	24	—	20	—

SM Higgs boson cross sections are multiplied by the $\mathcal{B}(a_1 a_1 \to \mu\mu bb)$ value that is calculated in the Type III model with $\tan\beta = 2$.

H → aa → 2b2μ/τ [2402.13358]

Table 2: Event yields in the $\mu\mu$bb channel for simulated processes and the number of observed events in data after applying $\chi^2_\mathrm{d} < 1.5$. The expected number of simulated events is normalized to the integrated luminosity of 138 fb^{-1}. The Type III parametrization of 2HDM+S with $\tan\beta = 2$ is used to evaluate $\mathcal{B}(\mathrm{a_1 a_1} \to \mu\mu\mathrm{bb})$.

Process	Yield
tt+jets	86.3 ± 2.2
DY ($10 < m_{\ell\ell} < 50$ GeV)	289.6 ± 89.5
DY ($m_{\ell\ell} > 50$ GeV)	200.2 ± 31.9
Diboson	1.5 ± 0.9
Single top	11.4 ± 1.6
Total expected background	589.1 ± 95.1
Data	641

Signal for ggH ($\mu\mu$bb)		
$m_{\mathrm{a}_1} = 20$ GeV	$m_{\mathrm{a}_1} = 40$ GeV	$m_{\mathrm{a}_1} = 60$ GeV
15.4 ± 0.2	18.7 ± 0.2	40.5 ± 0.3

H → aa → 2b2μ/τ [2402.13358]

In each category, subregions are defined using a threshold on the DNN score. The expected limits are scanned by varying the DNN thresholds to obtain the highest sensitivity to the simulated signal. This optimization method also ensures that the expected number of background events in each subregion is large enough to perform the final likelihood fit of the $m_{\tau\tau}$ distribution. There are three SRs for events containing one b jet: SR1, SR2, and SR3, whereas events with two b jets are divided into two categories: SR1 and SR2.

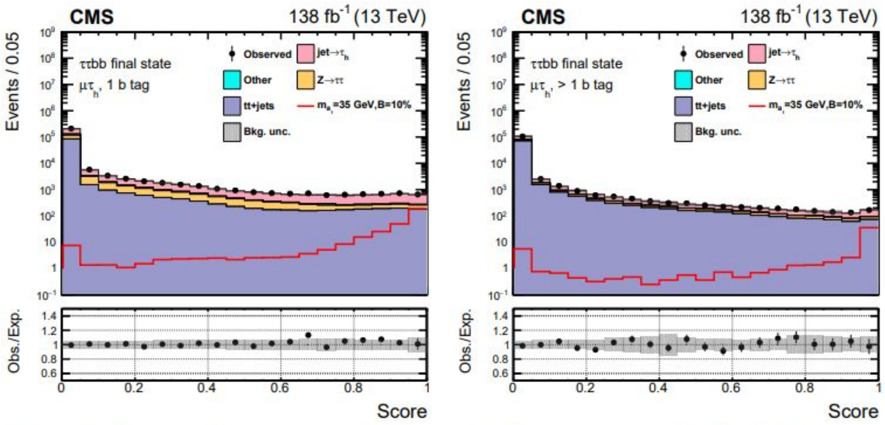

Figure 5: Pre-fit distributions of the DNN score for the $\mu\tau_h$ channel divided into events with one (left) or at least two (right) b jets. The shape of the $H \to a_1a_1$ signal, where $m_{a_1} = 35\,\text{GeV}$, is indicated assuming $\mathcal{B}(H \to a_1a_1 \to \tau\tau bb)$ to be 10%. The lower panel shows the ratio of the observed data to the expected yields. The gray band represents the unconstrained statistical and systematic uncertainties.

H → aa → 4μ [2407.20425]

We interpret the model-independent results in the context of several BSM benchmarks, including an axion-like particle (ALP) model [7, 13–16], a vector portal model with a dark scalar boson s_D [17–22], the next-to-minimal supersymmetric standard model (NMSSM) [6, 23–30], and supersymmetry (SUSY) models with hidden sectors (dark SUSY) [8, 22, 31]. In the ALP model [15], the SM-like Higgs boson, h, decays to the ALP, a, via $\mathrm{h} \to 2a$. The ALP then promptly decays into a dimuon. In the vector portal model, a massive dark vector boson Z_D decays to two new scalar bosons s_D, via $Z_\mathrm{D} \to s_\mathrm{D}\bar{s}_\mathrm{D}$, where we assume that the s_D is not self-conjugate, i.e., it is not equal to its antiparticle. The dark scalar boson s_D promptly decays to a dimuon. In the NMSSM, two of the three charge parity (CP) even, neutral Higgs bosons h_1 or h_2 (generically denoted $\mathrm{h}_{1,2}$) can decay to one of the two CP-odd neutral Higgs bosons a_1 via $\mathrm{h}_{1,2} \to 2a_1$. The CP-odd boson a_1 promptly decays to a dimuon. In the dark SUSY scenario, the breaking of a new $U(1)_\mathrm{D}$ symmetry gives rise to a massive dark photon γ_D. This dark photon can couple to SM photons via a small kinetic mixing parameter, ε. The proper decay length of the dark photon depends on its mass, m_{γ_D}, and ε. We use a signal topology where an SM-like h decays to the lightest non-dark neutralino, n_1, via $\mathrm{h} \to 2\mathrm{n}_1$. These neutralinos then decay via $\mathrm{n}_1 \to \mathrm{n}_\mathrm{D} + \gamma_\mathrm{D}$, where n_D is an undetectable dark neutralino. The dark photon γ_D then decays to a dimuon. Figure 1 displays the Feynman diagrams of the benchmark signal models.

NMSSM Dark SUSY

$H \to aa \to 4\mu$ [2407.20425]

Table 1: The event selection requirements for the 2017 and 2018 analyses. In the signal muon selection row, the particle-flow loose muons refer to those muons that have tracks in both the tracker and the muon system, which is contrasted with the standalone (SA) muon selection, which only requires tracks in the muon system.

Selection	Additional information	Requirement 2017	2018
Signal muon candidates	All 4 signal muons	4 PF loose muons	$\geq$3 PF loose muons and $\leq$1 SA muon
p_T ($\lvert\eta\rvert$)	All 4 signal muons	$p_T > 8$ GeV ($\lvert\eta\rvert < 2.4$)	$p_T > 8$ GeV ($\lvert\eta\rvert < 2.4$)
	2 signal muons	$p_T > 13$ GeV ($\lvert\eta\rvert < 2.0$)	$p_T > 24$ GeV ($\lvert\eta\rvert < 2.0$)
Invariant mass	Each dimuon	$m_{\mu\mu_{1,2}} < 60$ GeV	$m_{\mu\mu_{1,2}} < 60$ GeV
Fitted dimuon vertex probability	Each dimuon	$P_{\mu\mu_{1,2}} > 0.15$	$P_{\mu\mu_{1,2}} > P(L_{xy}, \Delta R, N_{SA})$
Dimuon isolation	Each dimuon	$\mathrm{Iso}_{\mu\mu_{1,2}} < 2.3$ GeV ($\Delta R < 0.4$)	$\mathrm{Iso}_{\mu\mu_{1,2}} < 2.3$ GeV ($\Delta R < 0.4$)
Fiducial volume	Each dimuon	—	$L_{xy} < 16.0$ cm $L_z < 51.6$ cm

H → aa → 4μ [2407.20425]

Table 2: The number of observed events in the CR and the expected and observed number of events in the SR in the three mass regions considered in this analysis.

Region	Quantity	Year 2017	Year 2018
Below J/ψ	Obs. events in CR	49	98
	Exp. events in SR	$2.26 \pm 0.32\,(\mathrm{stat}) \pm 0.14\,(\mathrm{syst})$	$4.34 \pm 0.44\,(\mathrm{stat}) \pm 0.18\,(\mathrm{syst})$
	Obs. events in SR	2	4
Above J/ψ, Below Υ	Obs. events in CR	2	66
	Exp. events in SR	$0.19 \pm 0.14\,(\mathrm{stat}) \pm 0.01\,(\mathrm{syst})$	$6.16 \pm 0.76\,(\mathrm{stat}) \pm 0.09\,(\mathrm{syst})$
	Obs. events in SR	0	6
Above Υ	Obs. events in CR	212	143
	Exp. events in SR	$18.10 \pm 1.23\,(\mathrm{stat}) \pm 4.49\,(\mathrm{syst})$	$13.81 \pm 1.16\,(\mathrm{stat}) \pm 5.39\,(\mathrm{syst})$
	Obs. events in SR	24	20

H → aa → 4μ [2407.20425]

Source of uncertainty	Value 2017	Value 2018
Experimental signal uncertainties		
Integrated luminosity	2.3%	2.5%
Muon ID	$4 \times 0.6\%$	$4 \times 0.6\%$
Dimuon isolation	$2 \times 0.1\%$	$2 \times 0.1\%$
Reco. of close muons in tracker (signal mass $<$ 9 GeV)	$2 \times 1.2\%$	$2 \times 1.2\%$
Reco. of close muons in muon system (signal mass $<$ 9 GeV)	$2 \times 1.3\%$	$2 \times 1.3\%$
Muon HLT	0.9%	0.6%
Reconstruction of displaced track/vertex	—	$2 \times 0.5\%$
PU distribution	0.1%	0.05%
PU effect on signal efficiency	2.3%	1.8%
Dimuon mass consistency	0.24%	0.24%
Experimental background uncertainties below J/ψ (0.21–2.72 GeV)		
Normalization	14.2%	10.1%
Systematic	6.6%	4.1%
Experimental background uncertainties above J/ψ and below Υ (3.24–9 GeV)		
Normalization	73.5%	12.3%
Systematic	5.9%	1.5%
Experimental background uncertainties above Υ (11–60 GeV)		
Normalization	6.9%	8.4%
Systematic	1.2%	2.3%
Shape	23.6%	36.7%
Theoretical signal uncertainties		
PDF + α_S + QCD scales	8%	8%
Higgs cross-section and BR[a]	3.8%	3.8%
NNLO Higgs p_T re-weighting[a]	2%	2%

[a]Uncertainty is not used in the vector portal model.

H → aa → 4b [2403.10341]

A multivariate discriminator based on a boosted decision tree (BDT) [65] is used to help separate signal and background events. Different BDTs are constructed for the WH and ZH channels, and the 3b and 4b event categories. The input variables for the BDT are:

- $p_{\mathrm{T}}^{\mathrm{H}}$: the vector sum of the transverse momenta of the three or four b-tagged jets forming the H boson candidate;
- m_{H}: the invariant mass of the three or four b-tagged jets forming the H boson candidate;
- $p_{\mathrm{T}}^{\mathrm{V}}$: for W boson candidates, the magnitude of the vector sum of the p_{T} of the electron or muon and $p_{\mathrm{T}}^{\mathrm{miss}}$; for Z boson candidates, the p_{T} of the dilepton pair;
- H_{T}: the scalar sum of the p_{T} of the three or four b-tagged jets that define the H boson candidate;

H → aa → 4b [2403.10341]

A multivariate discriminator based on a boosted decision tree (BDT) [65] is used to help separate signal and background events. Different BDTs are constructed for the WH and ZH channels, and the 3b and 4b event categories. The input variables for the BDT are:

- $p_{\mathrm{T}}^{\mathrm{H}}$: the vector sum of the transverse momenta of the three or four b-tagged jets forming the H boson candidate;
- m_{H}: the invariant mass of the three or four b-tagged jets forming the H boson candidate;
- $p_{\mathrm{T}}^{\mathrm{V}}$: for W boson candidates, the magnitude of the vector sum of the p_{T} of the electron or muon and $p_{\mathrm{T}}^{\mathrm{miss}}$; for Z boson candidates, the p_{T} of the dilepton pair;
- H_{T}: the scalar sum of the p_{T} of the three or four b-tagged jets that define the H boson candidate;

H → aa → 4b [2403.10341]

- $\langle \Delta R(\mathrm{b},\mathrm{b}') \rangle$: the separation in the η-ϕ plane between any two b-tagged jets in an event, averaged over all such combinations;
- $|\Delta\phi(\mathrm{V},\mathrm{H})|$: the azimuthal angle between the directions of the W or Z and the H boson candidates;
- $|\Delta\phi(j, p_{\mathrm{T}}^{\mathrm{miss}})|^{\mathrm{min}}$: the smallest azimuthal angle between the $\vec{p}_{\mathrm{T}}^{\mathrm{miss}}$ direction and a jet;
- p_{T}^{ℓ}: for WH events, the p_{T} of the electron or muon; for ZH events, the p_{T} of the leading electron or muon;
- $p_{\mathrm{T}}^{\mathrm{miss}}$: the magnitude of the missing transverse momentum;
- m_{T} (defined only for WH events): the transverse mass defined in Section 4;
- $\Delta m_{\mathrm{b\bar{b}}}^{\mathrm{min}} = |m_{\mathrm{b\bar{b}},1} - m_{\mathrm{b\bar{b}},2}|^{\mathrm{min}}$ (defined only for the 4b category): the minimum difference between two dijet masses formed from all possible combinations with the four b-tagged jets. The four b-tagged jets can be grouped in three different ways to form a pair of a $\rightarrow \mathrm{b\bar{b}}$ candidates. The $\Delta m_{\mathrm{b\bar{b}}}^{\mathrm{min}}$ variable represents the grouping that results in the smallest difference between the masses of the two pseudoscalar candidates.

H → XX → 4q [2407.09183]

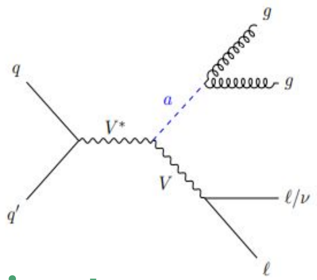

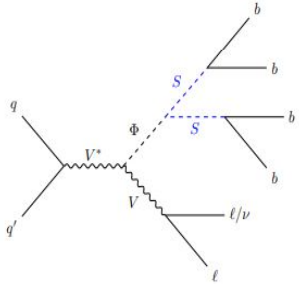

ATLAS EXPERIMENT

- LLP decaying in the **hadronic calorimeter.**
- Use of *calRatio* – HCAL to ECAL energy deposit ratio.

W associated

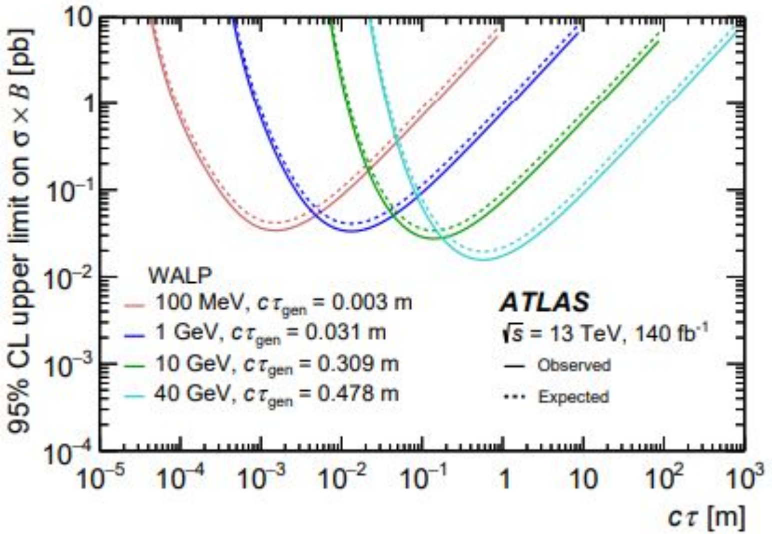

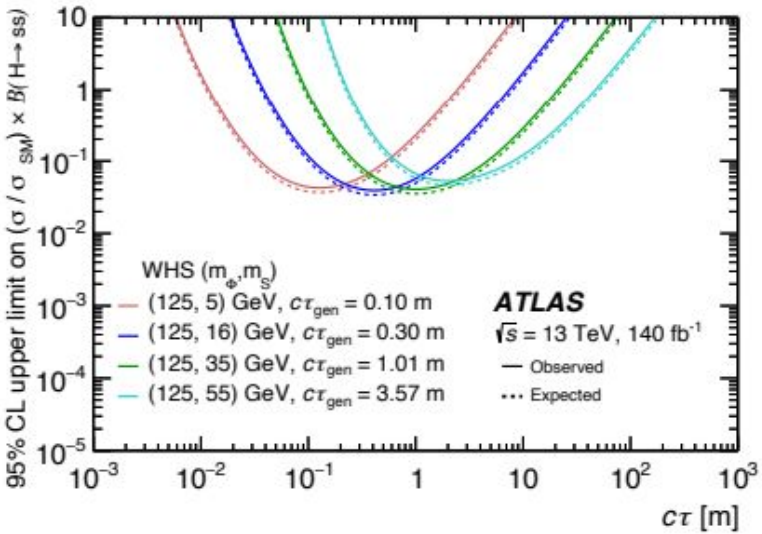

H → XX → 4q [2407.09183]

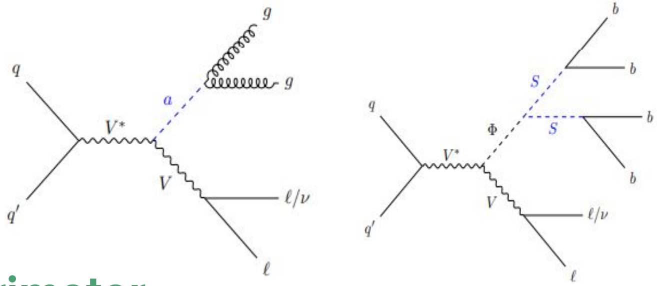

- LLP decaying in the **hadronic calorimeter.**
- Use of *calRatio* – HCAL to ECAL energy deposit ratio.

Z associated

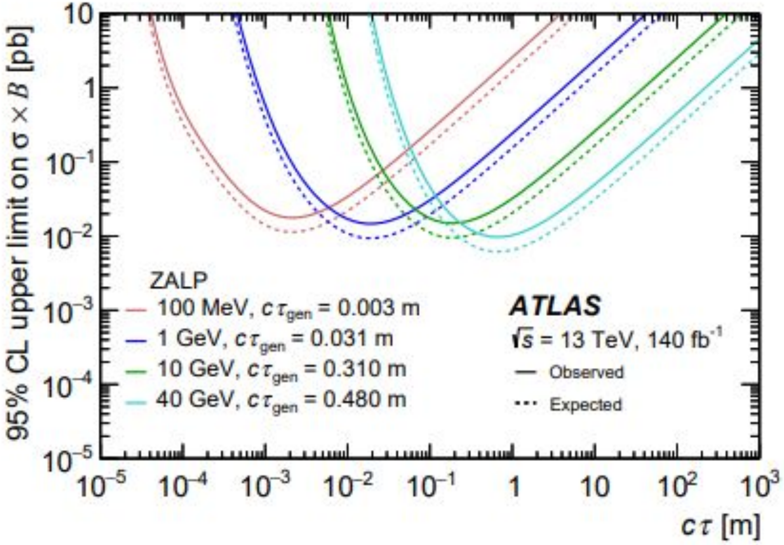

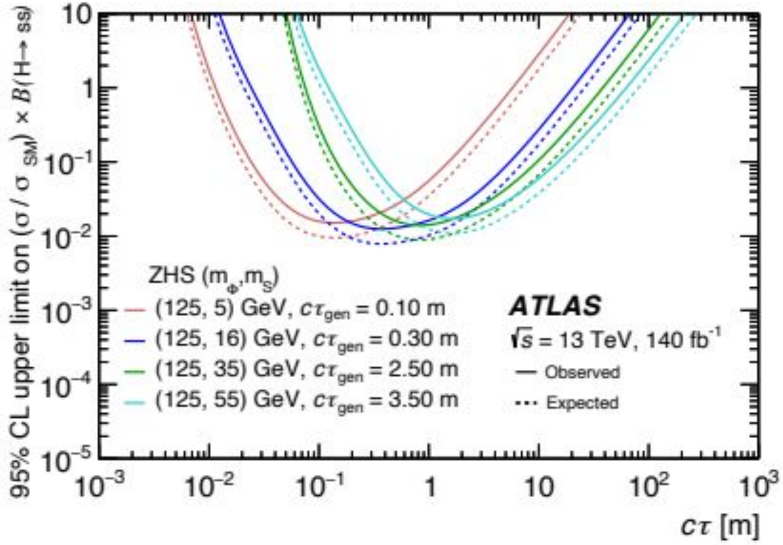

H → XX → 4q [2407.09183]

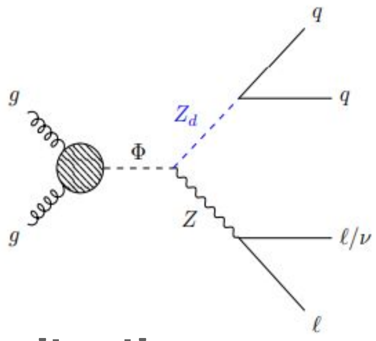

ATLAS EXPERIMENT

- LLP decaying in the **hadronic calorimeter.**
- Use of *calRatio* – HCAL to ECAL energy deposit ratio.

Z associated

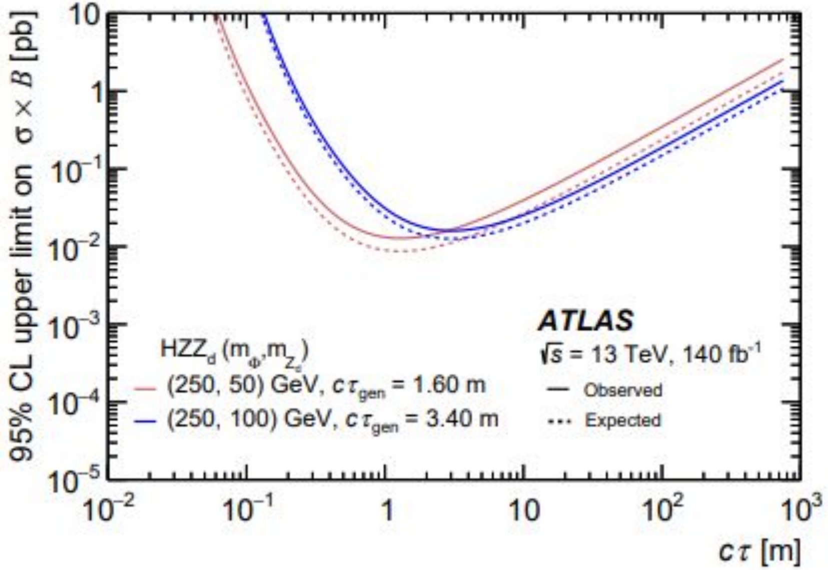

H → xx → 4q [2403.15332]

- LLP decaying in the inner detector.
- Use of displaced vertices, limits in various models.

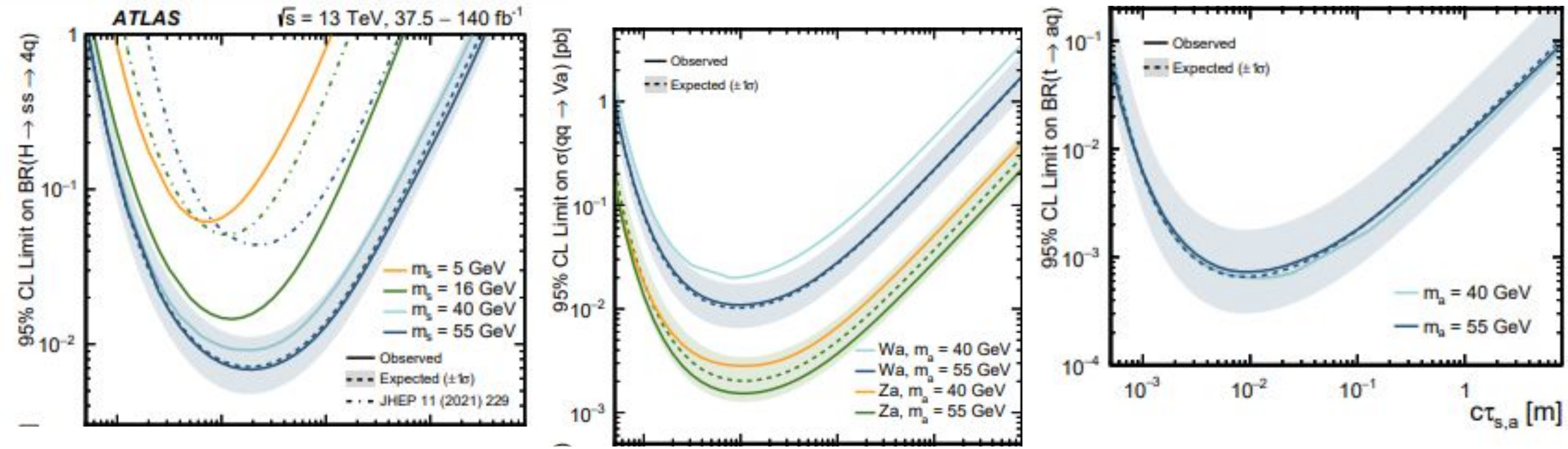

H → XX → 4q [2402.01898]

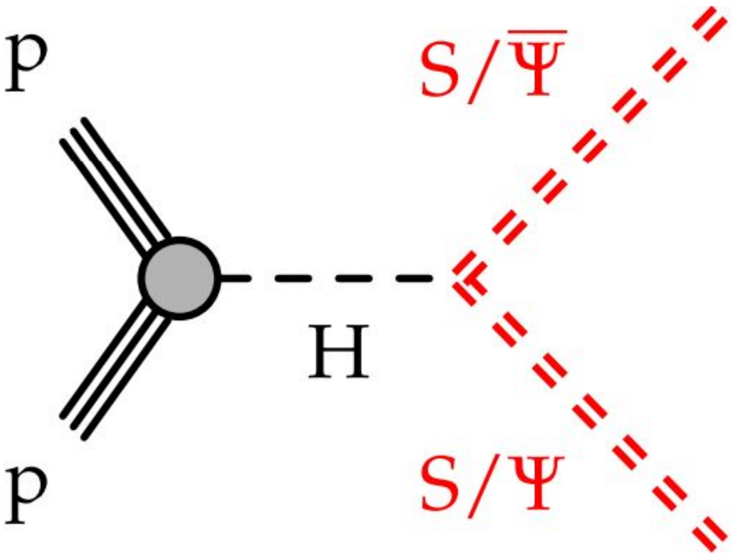

Search for LLPs using clusters in the MS

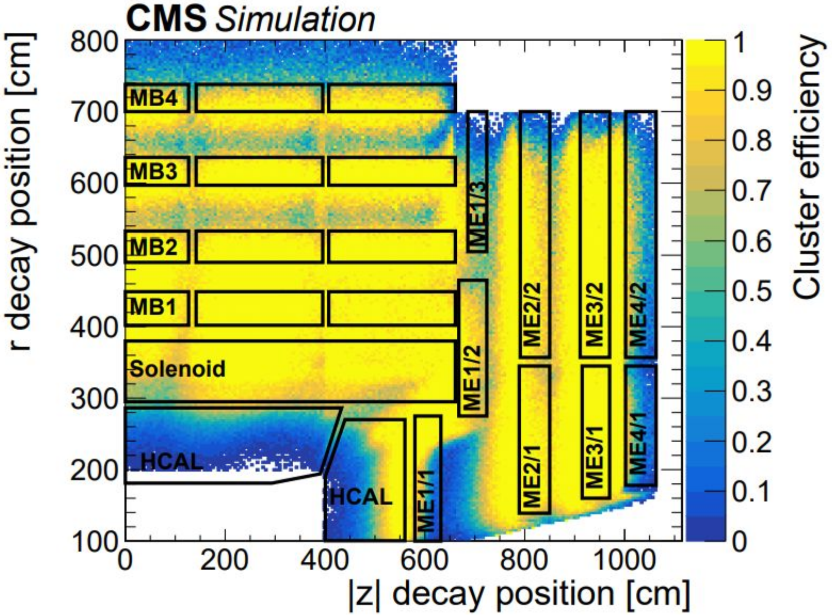

H → XX

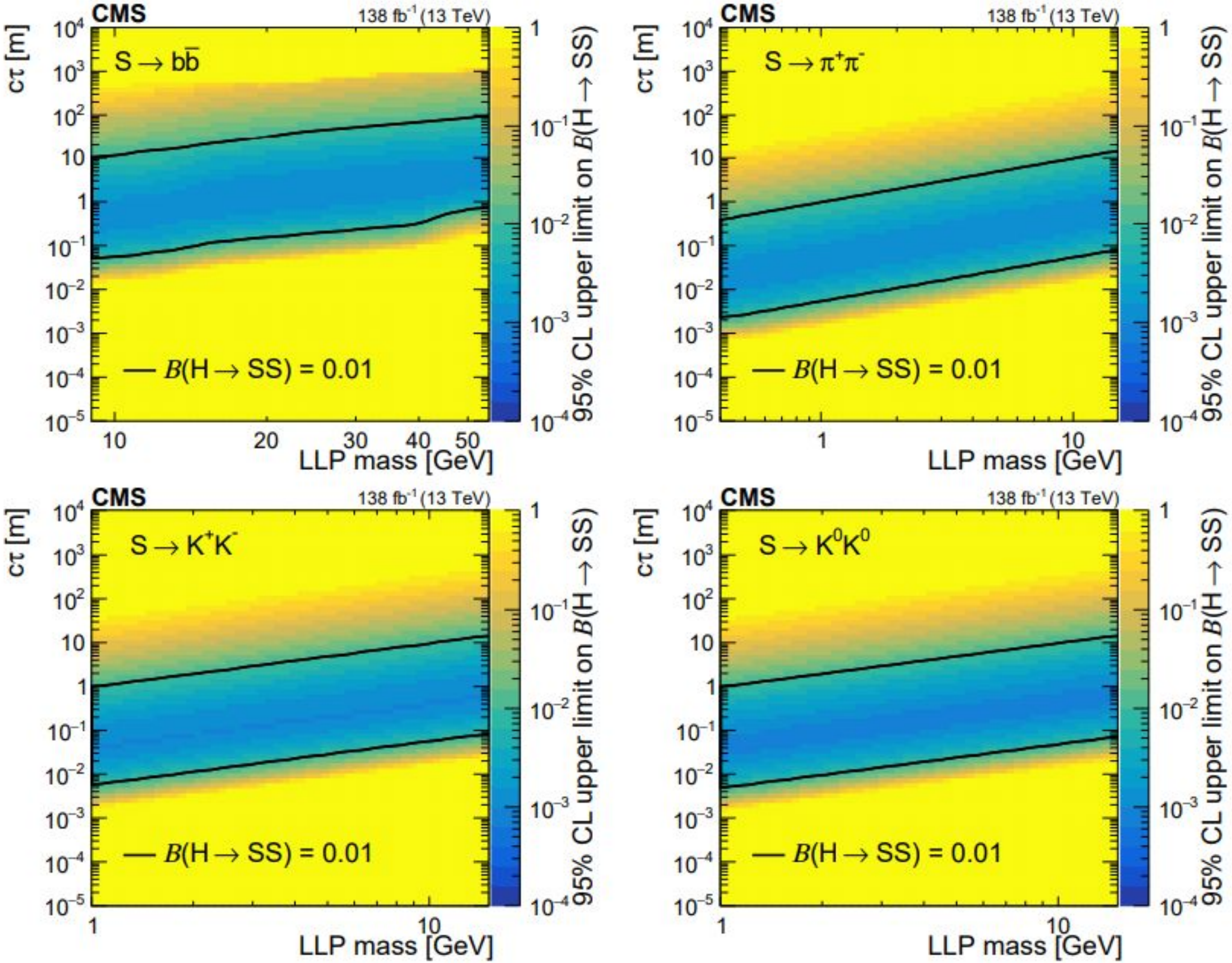

CMS
Compact Muon Solenoid

in the MS

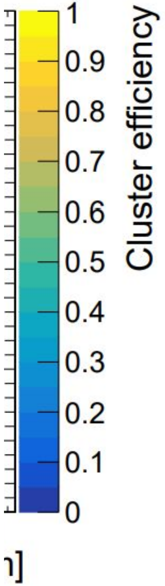

H → XX

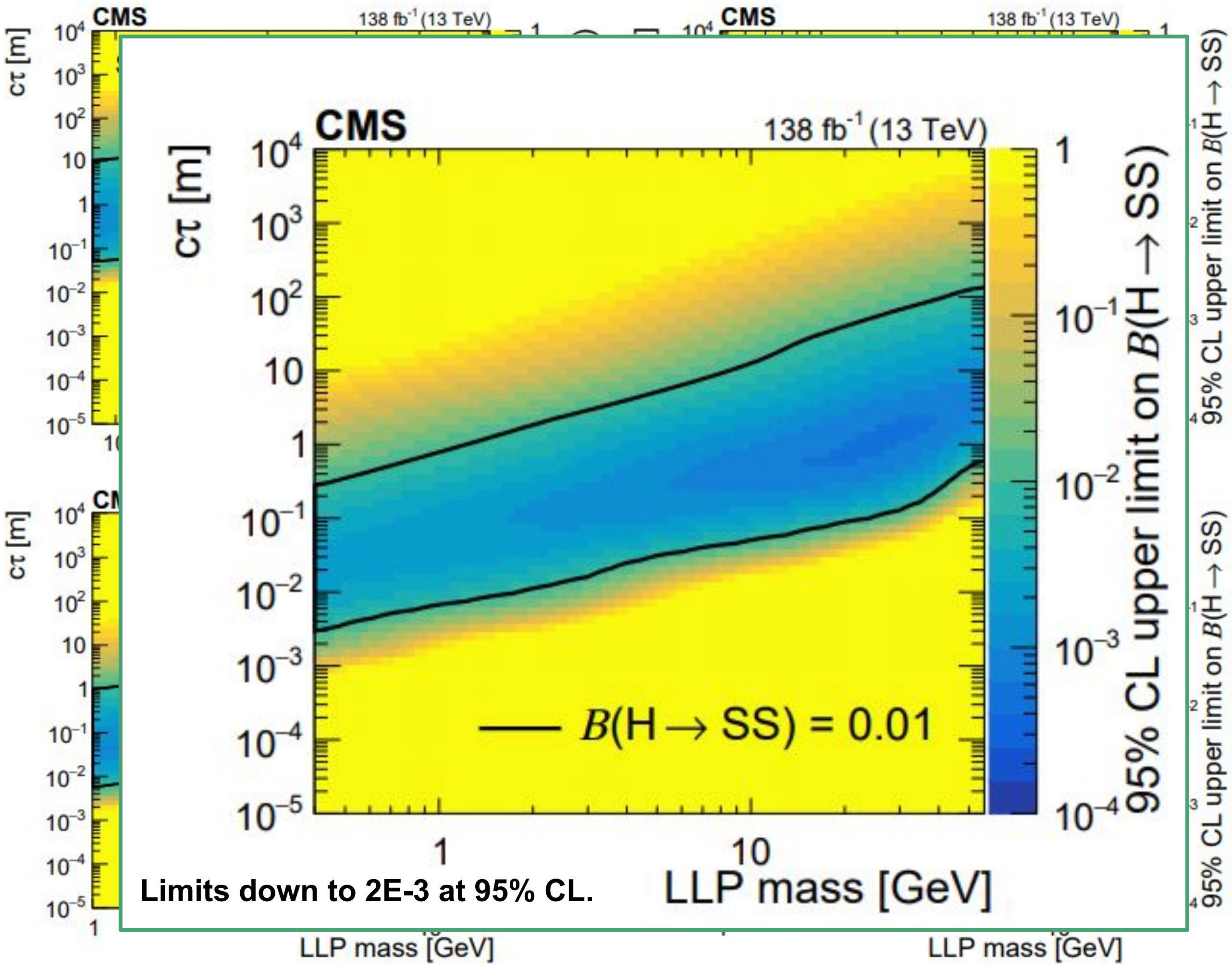

Limits down to 2E-3 at 95% CL.

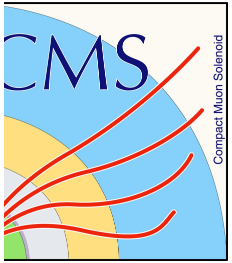

in the MS

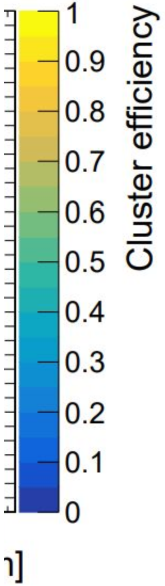

H → XX → 4q [CMS-PAS-EXO-23-013]

Novel techniques in trigger, reconstruction and machine learning → sensible improvement w.r.t. previous results!

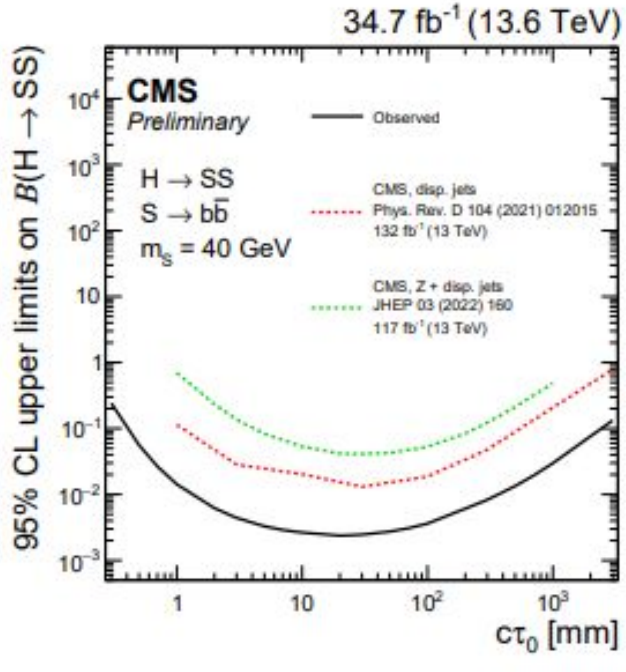

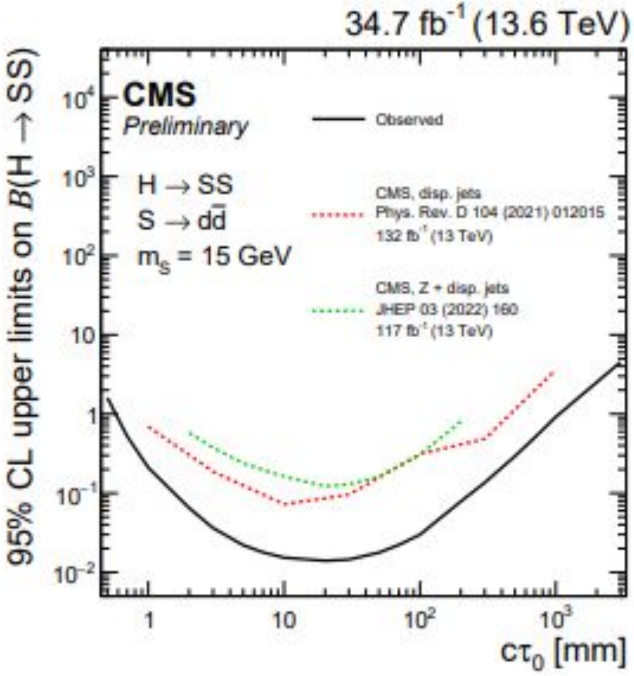

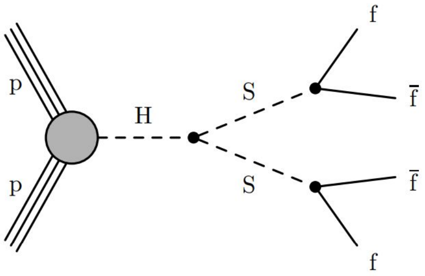

LLPs decaying into $e^+\mu^-\nu$ [EPJC (2021) 81 261]

Introduction:

- Search for a long-lived particle decaying into $e^+\mu^-\nu$, and produced:
  - via direct pair production (DPP) from pp collisions,
  - from an exotic Higgs decay (HIG), produced in pairs,
  - or from a charged current process (CC).

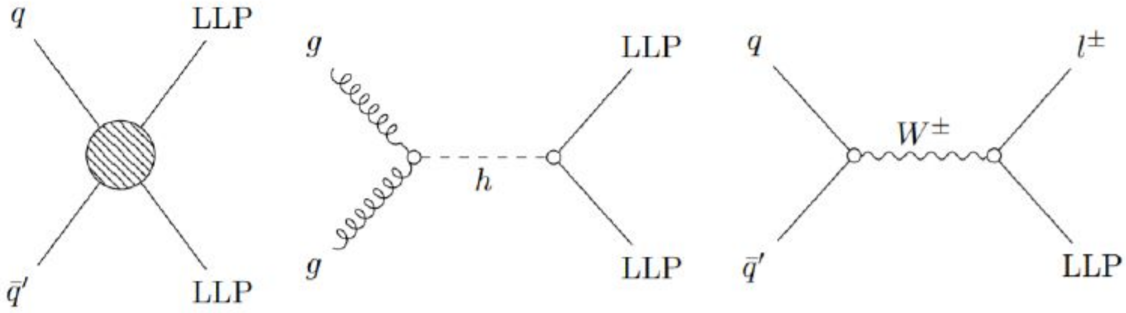

- LHCb Run 2 (2016 – 2018) dataset (5.38 fb^{-1} at 13 TeV).
- Explore masses between and 7 and 50 GeV and lifetimes between 2 and 50 ps.
- Leptonic triggers with low p_T requirements $\rightarrow$ allow to access small LLP masses.

LLPs decaying into $e^+\mu^-\nu$ [EPJC (2021) 81 261]

Simulation:

- Signal (DPP and HIG) using MSSM RPV model – LLP as $\tilde{\chi}_0^1$ light neutralino,
- Signal (CC) using LRSM model – LLP as a HNL from on-shell W boson decay,
- Several **signal samples** per model for different LLP mass and lifetimes.
- **Background sample** simulated for QCD $b\bar{b}$ events.

Selection:

- Require good quality DVs with minimum displacement and kinematic requirements.
- BDT with uniform boosting (response independent in mass) to purify signal sample.
- Two QCD categories: $e\mu$ from same jet ($\Delta R < 1$) or from different jets ($\Delta R \geq 1$).
- Leptons isolated to suppress QCD background – isolation optimised with same-sign data.
- After full selection $\rightarrow$ 60k $b\bar{b} \rightarrow e\mu X$ events (consistent with observed yield).

LLPs decaying into $e^+\mu^-\nu$ [EPJC (2021) 81 261]

Corrected mass approach:

- LHCb is a non-hermetic spectrometer $\rightarrow$ we **can not do invisibles.**
- However, we can compute a proxy to X+invisible invariant mass $\rightarrow$ **corrected mass**.
- **Required** to have only one **massless** invisible in the final state (ν).
- **Required** to know the **direction of flight** of the parent particle.

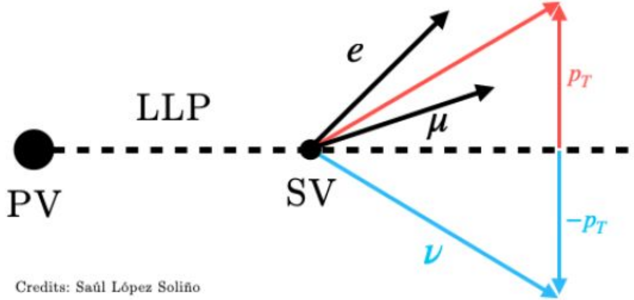

1. Assume LLP origin vertex approximately be the same as the pp collision.
2. Obtain a (pseudo) decay vertex using the di-lepton systems.
3. Project the di-lepton system momenta to the LLP direction of flight.

$$m_{\text{corr}} = \sqrt{m(e\mu)^2 + p(e\mu)^2 \sin^2\theta} + p(e\mu)\sin\theta$$

Corrected mass as a good proxy to real mass $\rightarrow$ discriminating variable.

LLPs decaying into $e^+\mu^-\nu$ [EPJC (2021) 81 261]

Results:

- Simultaneous ML fit to m_{corr} and LLP flight distance in two BDT bins.
- Backgrounds: Gaussian + Crystal Ball (ΔR <1) and Johnson SU (ΔR ≥1).
- Signal: modified Gaussian (left tail exponential, right tail power law) + Gaussian.
- Systematics dominated by choice of signal models.
- UL at 95% C.L. on σB per model – **no excess found**.
- Best UL for DPP with lifetimes below 10 ps and masses above 10 GeV → order of 0.1 pb.

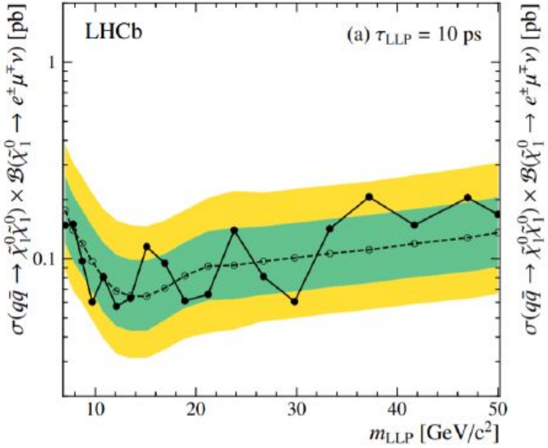

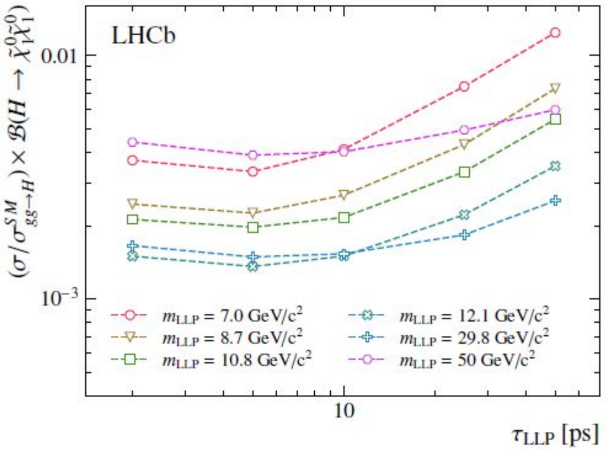

Massive LLPs decaying to jet pairs [EPJC (2017) 77:812]

- HV π_v decaying to $b\bar{b}$, especially SM-like $H^0 \to \pi_v \pi_v$ production.
- In most of the cases only one of the two π_v decays into the LHCb acceptance.
- Candidates are reconstructed using tracks originated within the VELO region.
- Experimental signature is a **single displaced vertex** with two associated jets:

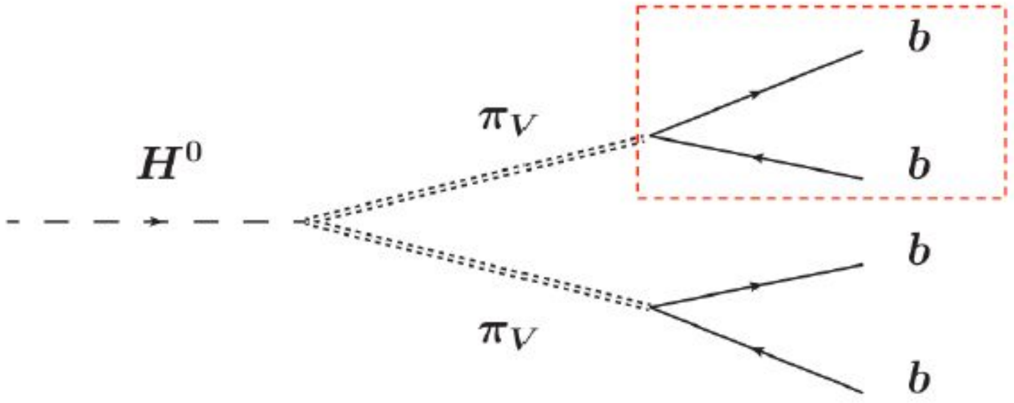

Massive LLPs decaying to jet pairs [EPJC (2017) 77:812]

- Efficiencies dominated by the detector acceptance (from 5.5% to 13%).
- Use π_v detachment (R_{xy}) to discriminate between signal and background.
- Background dominated by heavy flavour ($b\bar{b}$) events and material interactions.
- L0 trigger requires a high-p_{T} μ; **or** a h with high-E_T in the hadronic calorimeter.

Analysis procedure step-by-step:

1. Trigger on tracks passing a displaced vertex selection.
2. Reconstruct the displaced vertex and find two associated jets.
3. Quality cuts on jets – di-jet should point back to the candidate vertex.
4. Exclude material interactions + displaced vertices from heavy flavour (HF).
5. Fit the di-jet invariant mass in 6 bins of R_{xy} (0.4 – 50 mm).

Massive LLPs decaying to jet pairs [EPJC (2017) 77:812]

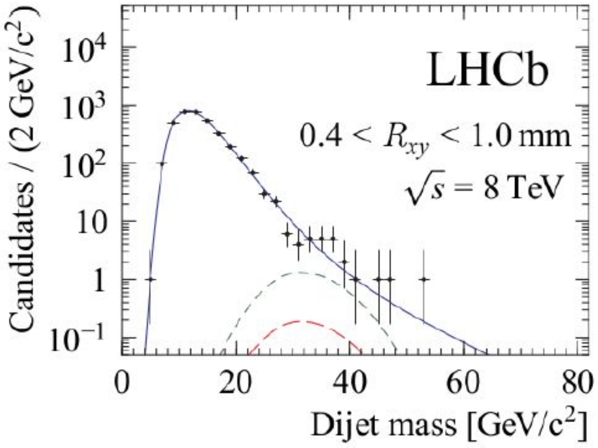

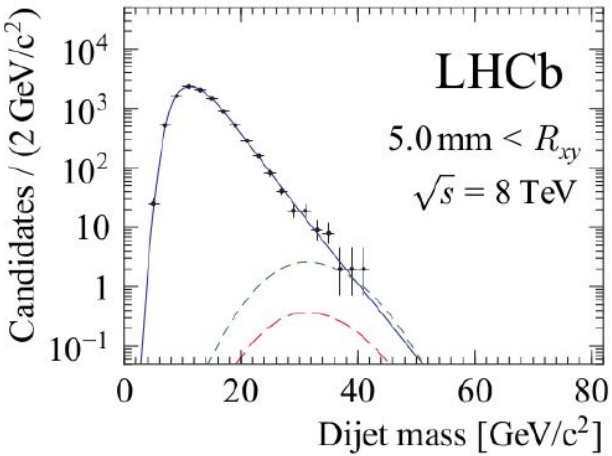

- Background model:
  - Material interactions with VELO sensors and envelope,
  - Heavy flavour ($b\bar{b}$) & back-to-back di-jet events.
- Signal model (35 GeV/c^2, 10 ps) for $\mathcal{B}(H^0 \to \pi_v \pi_v) = 1$.
- Best-fit signal model (35 GeV/c^2, 10 ps).

LLPs decaying into μ + jets [arXiv:2110.07293]

- **Massive LLP into μ + two quarks ($\rightarrow$ jets).**
- Signature sensitive to **several benchmark models:**
  - mSUGRA RPV neutralino,
  - Right-handed (Majorana) neutrinos,
  - Simplified MSSM production topologies:

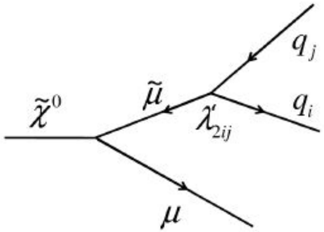

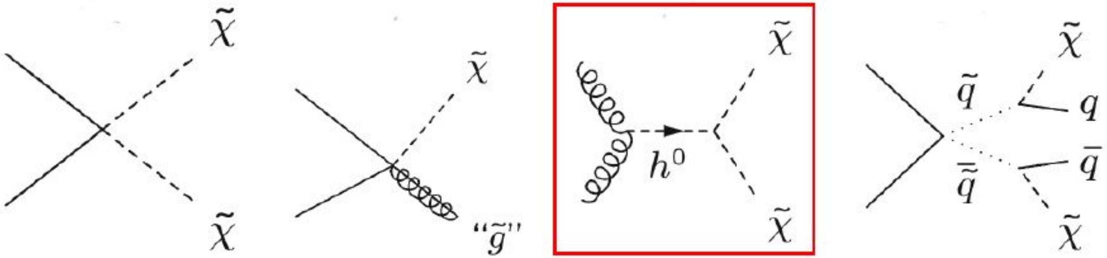

- One particular example: **decay of a Higgs-like particle** into two LLPs.
- Look for a **single displaced vertex** with several tracks + high p_T muon.
- Background dominated by $b\bar{b}$ events and material interactions.

LLPs decaying into μ + jets [arXiv:2110.07293]

- Search with 5.4 fb^{-1} of LHCb Run 1 and 2 data published.
- Results interpreted in $H^0 \to \tilde{\chi}_1^0 \tilde{\chi}_1^0$ benchmark model:

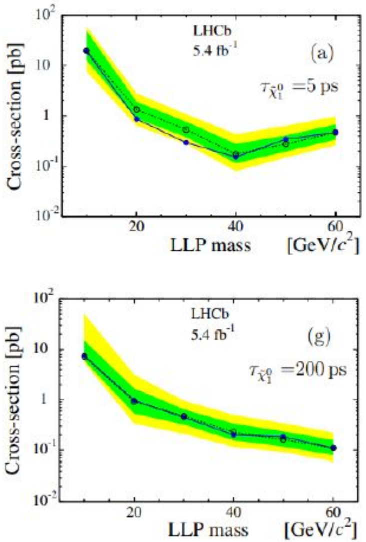

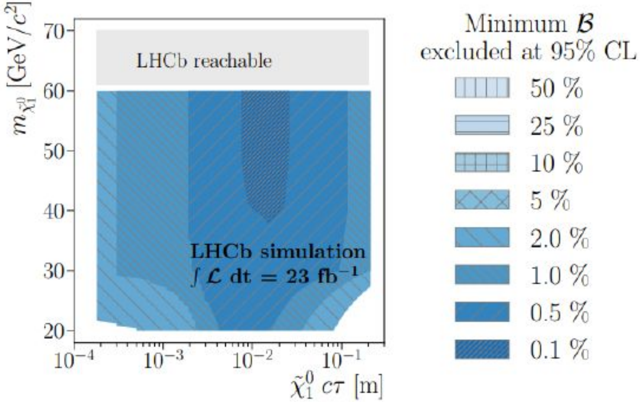

- Excluded production cross-section down to $\mathcal{O}(0.1)$ pb.
- Exclude $\mathcal{B}(H^0 \to \chi\chi)$ down to 0.1% by the end of Run 3 [LHCb-CONF-2018-006]

A COmpact Detector for EXotics at LHCb: CODEX-b

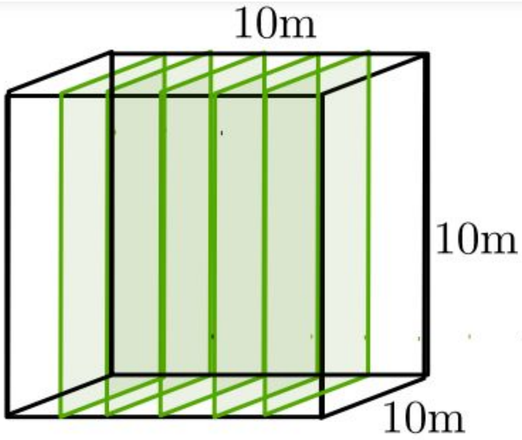

CODEX-b is a 10x10x10 m cube, with hundreds of **Resistive Plate Chamber (RPC) detectors** assembled in triplets and mounted in mechanical frames.

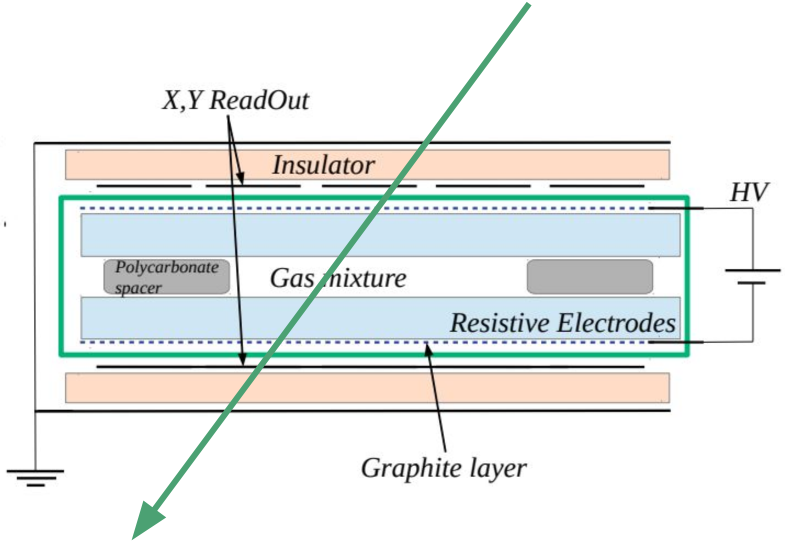

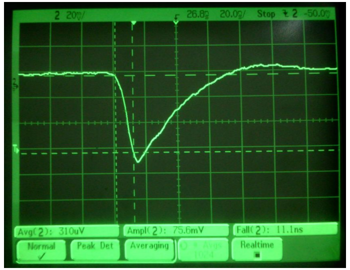

No civil work needed → will make use of existing facilities in the UXA85 cavern.

Relatively **cheap** detector, **O(10) M€**

Located 25 m away from the IP8 (LHCb).

Zero-background: UXA wall + shield veto.

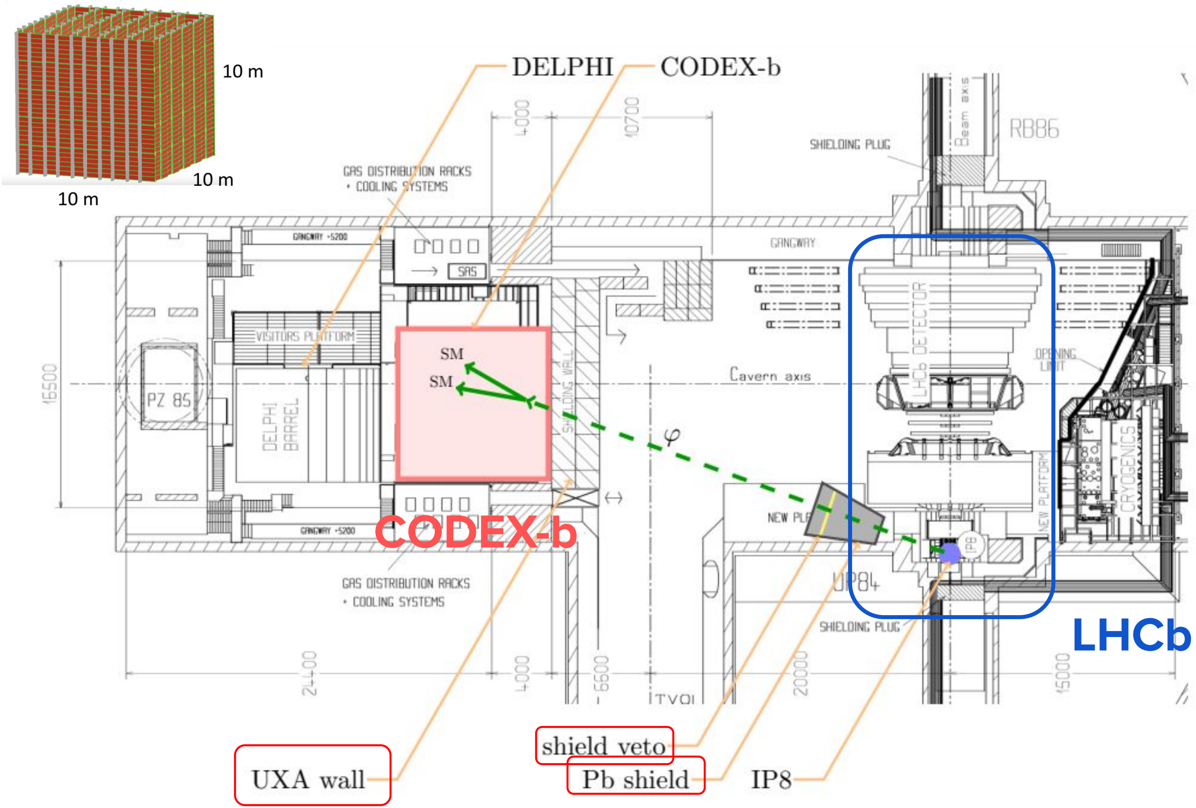

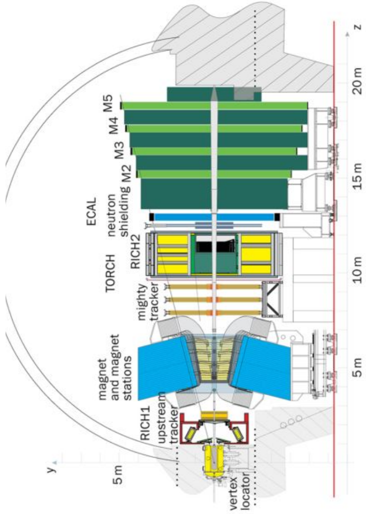

Reinterpretation with Delphes

JHEP 02 (2023) 011
Phys. Rev. D 108, 055040
JHEP 07 (2023) 079

- **MDS detector response is calorimetric**
  - Only depends on generator-level LLP hadronic energy, EM energy, and decay positions → release parameterized functions as supplementary materials on HEPData
- Integrated the CSC cluster detector response functions to Delphes: https://github.com/delphes/delphes/pull/103
- Recasted the analysis and projected sensitivity in a number of models: dark scalar, dark photon, ALPs, inelastic DM, hidden valley models, HNL, and VLL
  - These recasting efforts inspired the ongoing CMS analyses mentioned earlier

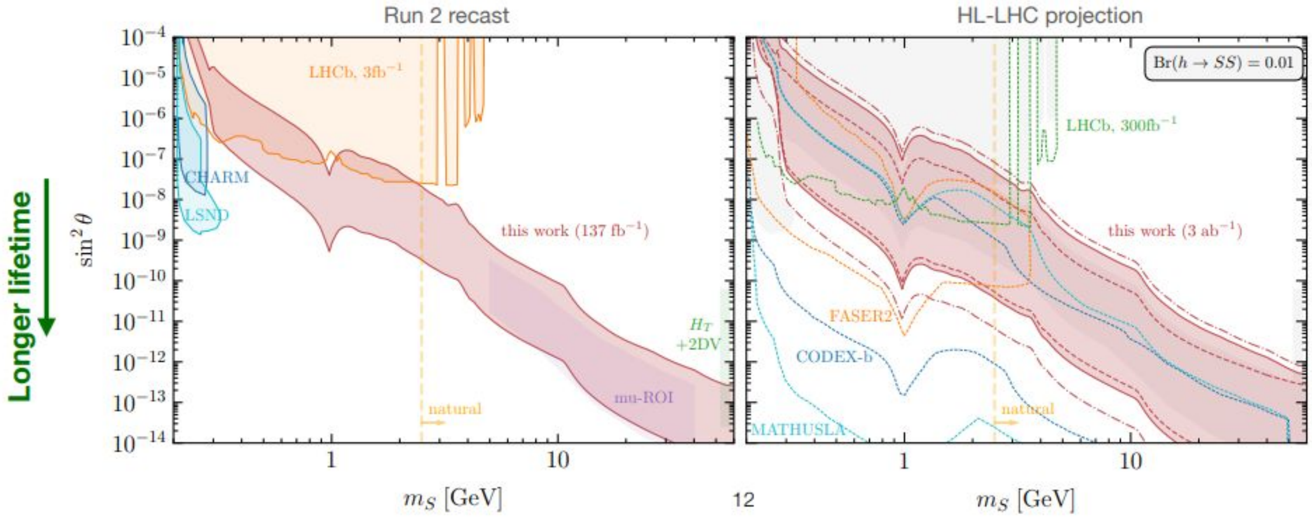

Dark scalar model

https://indico.cern.ch/event/1340162/contributions/5809466

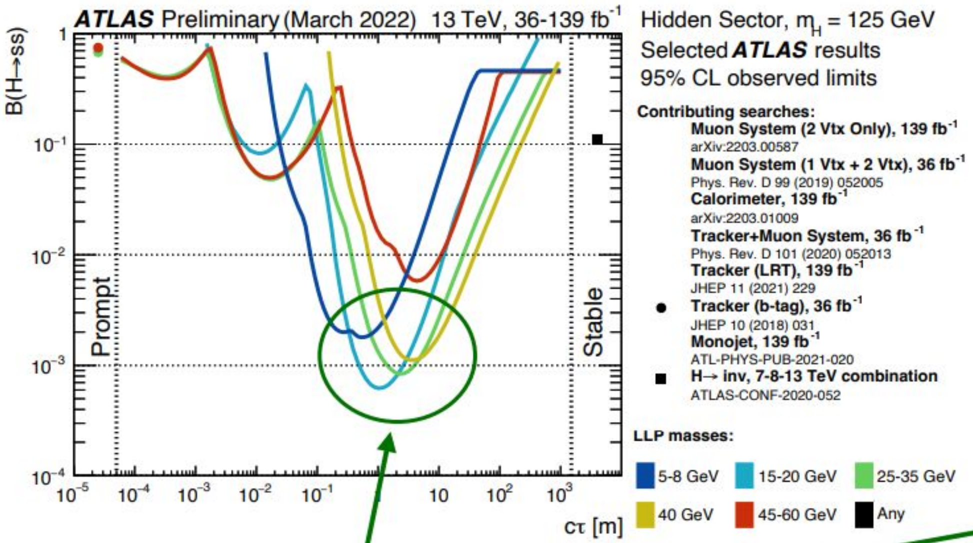

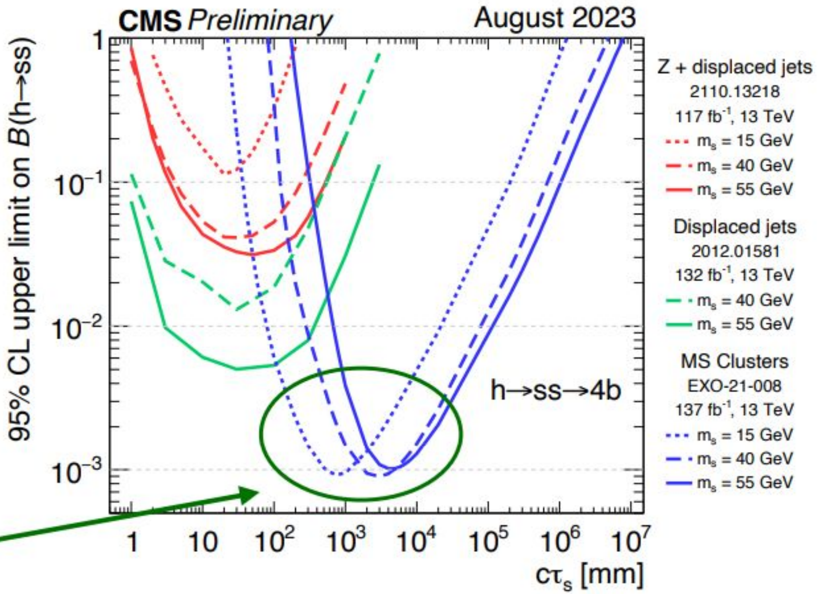

- Muon system analyses are among the most sensitive searches for both ATLAS and CMS

https://indico.cern.ch/event/1340162/contributions/5809466

arXiv:2311.00130

Associated production with a Z boson

138 fb^{-1} of Run 2 **CMS** data, search in **1 < m(a) < 30 GeV**.

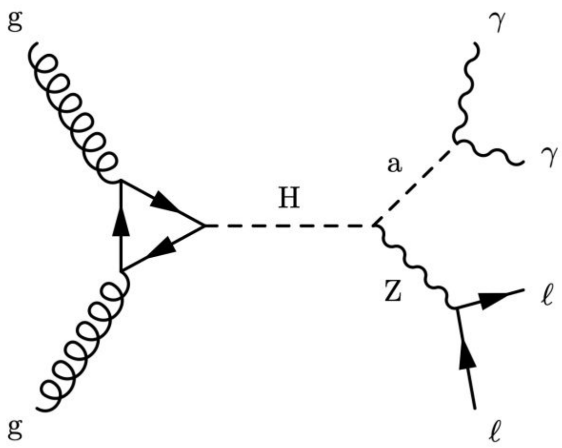

H→aZ, a→γγ, Z→ee/μμ

Signal simulated samples:

- **ggF H→aZ→γγll @ LO** (incl. leptonic τ decays),
- Steps of 1 (5) GeV in m(a) of 1-10 (10-30) GeV,
- Other production modes **negligible** after selection.

Background simulated samples: DY Z+jets @ LO, **jets** are **misidentified** as γ.

Leading μ(e) with **pT>20(25) GeV,** isolation with FSR recovery to exclude leptons from hadronic decays. **Photons** are required to have **pT>10 GeV.**

Za candidates require 95<m(llγγ)<180 GeV and ΔR(l,γ)>0.4.

arXiv:2311.00130

Associated production with a Z boson

Signal-to-background separation with **BDT uniform in m(llγγ)**, trained with pT, isolations, angular separations and calorimetry variables.

Unbinned ML fit to 95<m(llγγ)<180 GeV:

- **Signal**: n Gaussians (n<5) from MC,
- **Background**: Gaussian with falling spectrum function (turn-on-peak) of various functional forms.

Dominant systematic uncertainties: photon and **electron energy resolutions.**

Event categorization as a function of the BDT output:

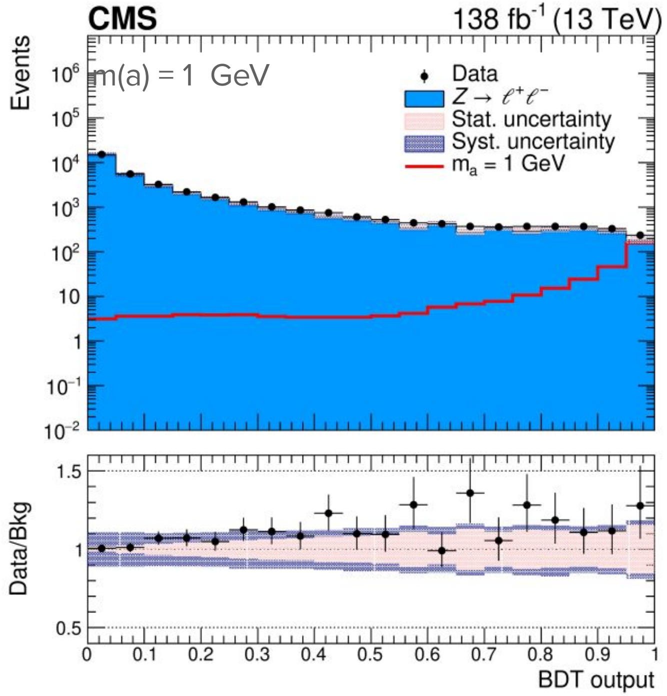

arXiv:2311.00130

Associated production with a Z boson

UL@95% CL on ZH eff. coupling with B(a→γγ)=1, and on production x-sections:

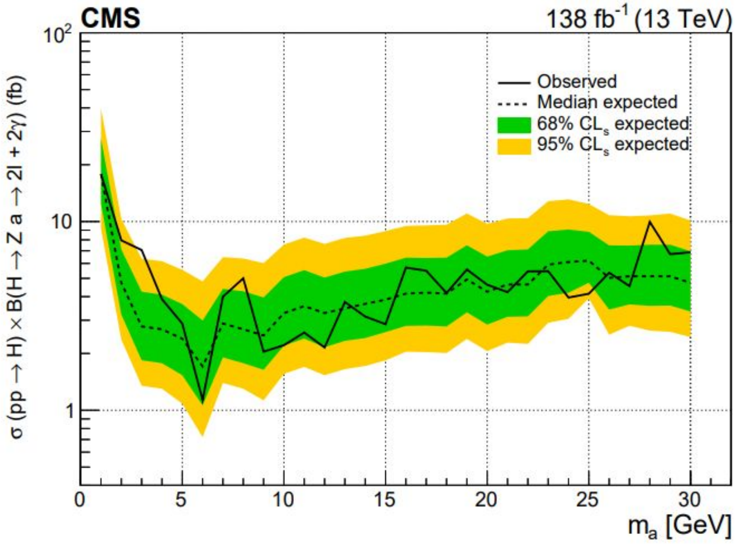

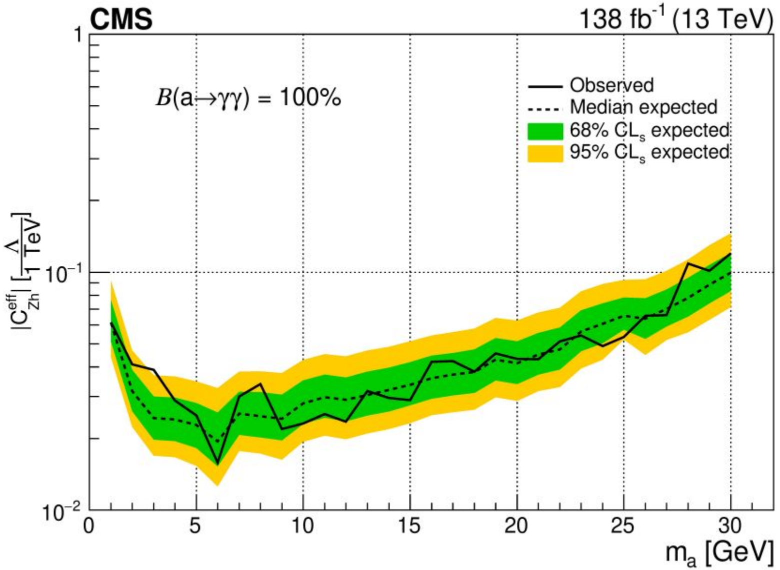

SM compatible, excess for m(a)=3 GeV of 2.6 (1.3)σ local (global) significance.